In presenting this thesis in partial fulfillment of the requirements for an advanced degree at Idaho State University, I agree that the library shall make it freely available for inspection. I further state that permission for extensive copying of my thesis for scholarly purposes may be granted by the Dean of the Graduate School, Dean of my academic division, or by the University Librarian. It is understood that any copying or publication of this thesis for financial gain shall not be allowed without my written permission.

Signature_______________________________________

Date____

Volcanic events and where to find them: Understanding and evaluating the volcanic vents and morphology surrounding Table Butte, a volcano on the eastern Snake River Plain

By

Shanon J Wilmot (Brailsford)

A thesis

Submitted in partial fulfillment

Of the requirements for the degree of

Master of Science in the Department of Geosciences

Idaho State University

Spring 2022

The members of the committee appointed to examine the thesis of Shanon J Wilmot find it satisfactory and recommend that it be accepted.

Shannon Kobs Nawotniak

Major Advisor

Kendra Murray

Committee Member

Robert Watkins

Graduate Faculty Representative

DEDICATION

This thesis is dedicated to the multitude of people who supported me. Primarily, Talia, my daughter, you will never understand the support I received just by coming home to you or receiving a hug. Your hugs are the best and always encourage me to do my best and live my life to the fullest each day. When I needed you, my dearest friends Alexis, Kaitlyn, and Chandra, or you saw that I needed you, one of you always showed up. These three always reassure me and encourage me to keep going even when I am at my lowest. I also want to dedicate my work to all the women working to reach the stars and climb their mountains. Even when all the odds are against them. You are beautiful. You are strong. You got this. Then last but not least, my family, for the multitude of times that I received help with babysitting, laughter, encouragement, and love. I genuinely appreciate you all, and I will never forget.

ACKNOWLEDGMENTS

I need to express my gratitude to Shannon Kobs Nawotniak and Kendra Murray. Thank you for all the time, knowledge, guidance, and insight shared with me to achieve my goals with my education. I will never forget how passionate you are about science and helping your students succeed. Also, thank you for your added patience with my lack of knowledge and post-surgery successes and failures that impeded my progress. Finally, I cannot thank you enough for your support with me.

I could not have done this research without my “Uncles”: William Hackett, Duane E. Champion, and Scott Hughes. Not only did they recognize my potential and ability to apply GIS tools to the project. They knew the need for the research to be completed and created the research project, and they would always be willing to meet with me and answer any questions I had. I would not have achieved this research without them. Thank you for taking me under your wing and helping me to succeed.

I also want to thank H. Carrie Bottenberg, David Pearson, Paul Link, and Jerad Anderson for pushing me to become a geologist and GIS professional before I even had a bachelor's degree and encouraging me to succeed even when I did not think I could.

This work could not have happened without the support of Robert Watkins, Mel Kuntz, Glenn Russell, Keith Weber, Mike McCurry, and their officemates.

A special acknowledgment and thank you goes to Kathleen Van Wesenbeeck for all your hard work and understanding of the importance of my thesis work. In addition, I cannot express my gratitude enough for helping me with my fieldwork when I had physical limitations. Finally, I would also like to thank E. Chase Porter, Lindsey Sutherland, Rituraj Yadav, Virginia Valvold, and Thane Kindred for their unwavering support and help with the research and writing of this research paper.

Lastly, I would like to thank my family and friends that extend across the world and believe in me. I faced challenges in many facets of my life during the process of earning a Masters's degree. However, I could not have accomplished my goals without you. I will never forget how thankful I am to all of you.

This work was funded by the Idaho National Laboratory through the U.S. Department of Energy Idaho Operations Office contract DE-AC07-05ID14517. In addition, I acknowledge the Analytical Geochemistry Lab at Brigham Young University for x-ray fluorescence analysis and Texas Petrographic for the production of thin sections.

Table of Contents

List of Figures

List of Tables

List of Abbreviations/Symbols

ESRP	Eastern Snake River Plain
INL	Idaho National Laboratory
PVHA	Probabilistic Volcanic Hazards Assessment
BEA	Battelle Energy Alliance
SSHAC	Nuclear Regulatory commission’s Senior Seismic Hazards Analysis Committee
NDCA	New Data Collection and Analysis
KDE	Kernel Density Estimation
NAIP	National Agricultural Imagery Project
GPS	Global Positioning Systems
ISU	Idaho State University
XRF	X-ray fluorescence
USGS	United States Geological Survey
Qtbb	Quaternary Table Butte basalt

Volcanic events and where to find them: Understanding and evaluating the volcanic vents and morphology surrounding Table Butte, a volcano on the eastern Snake River Plain

Thesis Abstract – Idaho State University (2022)

Table Butte is an anomalously shaped volcano found on the eastern Snake River Plain in Idaho. The main volcanic edifice has steep sides and a flat top, while linear groupings of craters and mounds, known as The Breaks, are located immediately to the south and west. The large number of vents currently mapped at Table Butte has long been considered suspect, with concerns that the craters associated with the linear clusters could be secondary vents from littoral blasts, a hypothesis given weight by phreatomagmatic ejecta deposits observed in the area. This research is the first thorough investigation of Table Butte and has the primary objective of determining how many vents and events are represented at the location. Using a combination of fieldwork, petrographic analyses, and geochemical data, I identified 18 vents, split across two events. While The Breaks included some phreatomagmatic tephra deposits, they were dominated by welded spatter from fissure fountaining. There was no observable phreatomagmatic evidence on the main edifice itself, leaving the question of the unusual morphology unresolved. We currently hypothesize that the steep sides and flat top were caused by a buried unit that experienced some form of phreatomagmatism during eruption and was subsequently buried by dry lava flows. While it is possible that the morphology could also be related to a cryptodome, we do not favor this hypothesis based on the orientation of lava flows, lack of extension cracks, and consistency of paleomagnetic inclination measurements taken from the top and slope of the main edifice and associated lava in The Breaks. We interpret that the first event occurred along the Needle Butte trend and north-south portion of The Breaks with the eruption of a plagioclaserich lava. Later, an olivine-rich lava erupted into external water and eventually transitioned to a dry eruptive environment, mantling the original steep-sided landform.

Keywords: Table Butte, Eastern Snake River Plain, Volcanic Vents, Distributed Volcanism,
Kernel Density Estimations

Chapter 1: Introduction

1.1- Overview

The eastern Snake River Plain (ESRP), a distributed basaltic field and the type location for plains-style volcanism, is essential for understanding the geologic history and volcanic hazards of Idaho (e.g., Bonnichsen et al., 2002; Gallant et al., 2018; Greeley, 1982; Hughes et al., 1999) and for studying planetary volcanism by terrestrial analog (e.g., Hughes et al., 2019; Neish et al., 2017; Tolometti et al., 2020). While accurate maps of past volcanism are critical to evaluating the potential for future eruptions and associated hazards, there are areas of suspected inaccuracies in the existing ESRP maps, including Table Butte (Fig. 1.1) (Hughes et al., 2002).

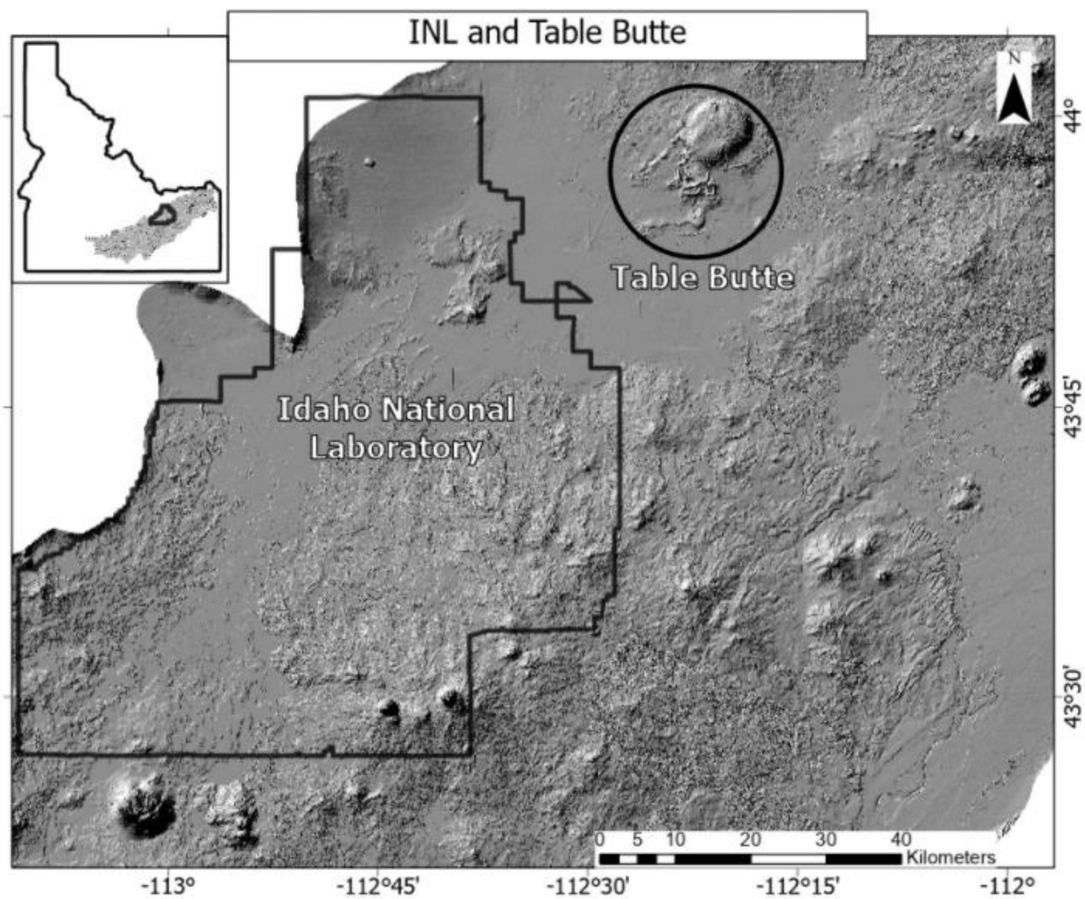

Figure 1.1: Regional hillshade map of the ESRP (USGS) with the Idaho National laboratory and the Table Butte study area included.

Unlike most of the volcanoes on the ESRP, Table Butte has a steep-sided and flat-topped central platform, ejecta deposits including lake sediment blocks (S. Hughes, *personal communication*), and ~25 small craters (Wetmore et al., 2009; Gallant et al., 2018). These features suggest that phreatomagmatic eruptions may have partially formed Table Butte. Consequently, many of the craters previously mapped as vents from aerial imagery (Wetmore et al., 2009) may represent rootless steam explosion pits; while Hughes et al. (2002) indicated that they suspected that vent maps of Table Butte were incorrect, there has been no subsequent study to differentiate between primary and rootless vents. Incorrectly labeling such features creates a problem with existing ESRP maps and datasets because rootless vents and primary vents are fundamentally distinct features and should not be conflated (Wohletz, 1986). Incorrectly identified primary vents, particularly ones in a cluster like at Table Butte, have the potential to strongly influence calculations of eruption frequency, lava volume over time, and probability of inundation in the future. Multiple vents can erupt simultaneously or in quick succession from the same magma reservoir, resulting in a singular event composed of multiple vents (e.g., Deng et al., 2017; Gallant et al., 2018; Grosse et al., 2020; Wetmore et al., 2009). As such, it is essential to correctly identify the eruption history of Table Butte and differentiate between rootless vents and primary vents.

Further, unpublished paleomagnetic data suggest that Table Butte erupted as a singular event (D. Champion, *unpublished data*). The paleomagnetic data has potentially profound implications for the probability of future volcanic events in that area. Consistent inclination and declination values across the Table Butte area suggest emplacement during a singular event; however, the paleomagnetism samples were taken without the benefit of detailed field mapping and may not actually represent different geologic units. In fact, there is a possible divide in the main edifice, with topographic indicators suggesting that the northern portion of Table Butte and the Needle Butte trend could have been emplaced in a separate event from the southern main edifice and The Breaks.

Based on topography, satellite imagery, unpublished paleomagnetism data and un-georeferenced photos of tephra deposits taken during a field trip taken approximately 20 years ago, I hypothesized that:

- H1: Table Butte initially erupted subaqueously and transitioned into a subaerial eruption.
- H2: Most of the currently mapped vents of Table Butte are rootless, and there are only four primary vents.
- H3: The Table Butte system was emplaced over multiple events.

1.2- Study Area

The ESRP is a monogenetic, plains-style volcanic province containing small basaltic shield volcanoes (Greeley, 1982; Hughes et al., 2002). The Yellowstone hotspot's passage forms the ESRP, which spans 350 km x 100 km from Twin Falls to Ashton, Idaho. The area continues to be active, with basaltic eruptions as recent as ~2 ka (Kuntz, 1979,1992; Kuntz et al., 2003, 2007, 2018; Skipp and Kuntz, 2009). ESRP volcanism spans a wide compositional range. Although tholeiitic basalts make up most of the lava, there are several rhyolitic domes along the plain's central axis, and intermediate compositions are observable in a few locations such as Craters of the Moon and Cedar Butte (e.g., Hughes et al., 1999; Morse, and McCurry, 2002; McCurry et al., 2008). In addition, hundreds of tholeiitic vents dot the ESRP, with possible vent corridors providing evidence of regional extension (Hughes et al., 2002). Though small shield volcanoes are the most common edifice type on the ESRP, collapsed craters, lava lakes, tuff cones, scoria cones, fissures, and domes (Greeley, 1982). Greeley (1982) introduced plains-style volcanism to describe a hybrid of flood basalts and low shield volcanoes. Plains-style volcanism exhibits <10 m thick lava flows that spread over five km to 20 km depending on the volume of basalt. The newer eruption then flows over older volcanics after erupting from central vents; this creates a series of overlapping low shield volcanoes and fissures (Greeley, 1977, 1982).

Distributed volcanic fields are characterized by edifices, typically shields or cones, that only erupt once. Of the >500 vents currently mapped on the ESRP, most are considered monogenetic (e.g., Gallant et al., 2018; Wetmore et al., 2009), including the seven volcanoes that erupted during the last 12 ka: Shoshone, Kings Bowl, Wapi, North and South Robbers, Cerro Grande, and Hells Half Acre (Kuntz et al., 2003). In addition, the spatial distribution of vents indicates that eruptions are not time-transgressive across the ESRP (Armstrong et al., 1980), meaning that the next eruption could occur anywhere within the existing ESRP boundary.

Although more than 25 vents have been mapped in the Table Butte area (e.g., Hughes et al., 2002; Gallant et al., 2018; Wetmore et al., 2009), many of those locations were interpreted from aerial imagery, DEMs, and topographic maps (Gallant et al., 2018; Wetmore et al., 2009; W. Hackett, *pers. comm.*). Many of the mapped vents occur in linear clusters to the south and west of the main Table Butte edifice and may be rootless vents, that is, small craters formed in a lava flow by steam explosions when the lava flows over wet ground (Hughes et al., 2002). The Table Butte complex covers an area of 42 km^2, with a local vent density of ~0.6 vent/km^2 using the Hackett et al. (*in prep*) vent map. Other shield volcanoes on the ESRP with similar footprints only have one or two vents (~0.02-0.06 vents/km^2). The large difference between the apparent vent density at Table Butte and nearby ESRP shield volcanoes makes emphasizes the need to understand the number of true vents and events in that area to determine whether there are unique volcanic processes and hazards represented there.

Other influences on the ESRP include phreatomagmatism, an interaction between magma and external water during the eruption that resulted in increased explosivity (e.g., Morrissey et al., 2000). Unpublished photos taken at Table Butte suggest zones of tephra blast deposits, including lacustrine blocks in some areas, while other regions have lava flows (Fig. 1.2) (S. Hughes, *per. comm.*). These features would suggest a transition from subaqueous to subaerial eruption styles as the volcano grew. In addition, there is geologic evidence of lakes in the Table Butte area throughout time, including 17 ka to the present (Gianniny et al., 2002); although there is no documented lake there ~400 ka, the recurrence of surface water in the area and the existence of a shallow aquitard holding up a perched aquifer (Spinazola, 1994) suggest that the site may have been adequately wet to induce phreatomagmatism at the time of the eruption(s).

Figure 1.2: Photographic evidence of phreatomagmatic deposits in the Table Butte area (Lat: 43° 55’ 29” N. Long: 112° 21’ 04” W.). Photo courtesy of S. Hughes.

1.3- Research Goals and Objectives

Table Butte's geologic history, particularly the number of vents and events and the interaction with external water, will provide crucial details applicable to hazard analysis in the area. In particular, the results of this work will contribute to improved probabilistic volcanic hazard analysis for INL.

Hypothesis One: Table Butte initially erupted subaqueously and transitioned into a subaerial eruption.

Old field photos indicate that Table Butte has at least some outcrops that include tephra deposits consistent with phreatomagmatic blasting. The outcrops display lacustrine sediment and volcanic rip-up clasts that came from the explosive emergence of the lava through a lakebed. Lava flows pictured in other areas of Table Butte indicate that there were also periods of dry eruptions. These particular spatial patterns of phreatomagmatic and subaerial deposits signify a water source that influenced Table Butte eruptions, though the lack of spatial data attached to the photos makes it difficult to interpret whether the wet-dry shift is associated with lateral or vertical growth of the volcano. Lakes have existed in the area for thousands of years, so it is plausible that there was a shallow surface or subsurface water source in the area during the eruption of Table Butte. Quenched fragmented basalt clasts and associated ejecta deposits, possibly including palagonite, would provide evidence in support of a region having explosive interaction between molten rock and external water; similarly, the distribution of such evidence throughout the field area would indicate when such eruptions occurred relative to units that do not demonstrate water interaction, thereby allowing us to determine whether the construction of Table Butte transitioned from wet to dry, dry to wet, or some other sequence associated with space and time (Wohletz and Sheridan, 1983). This hypothesis is assessed primarily through field mapping dry and wet facies and identifying their timing relative to the overall volcanic history of Table Butte.

Hypothesis Two: There are fewer vents than previously mapped, with perhaps as few as only five primary vents.

Previous maps of Table Butte (Kuntz et al., 1994; Kuntz, *unpublished*) indicate 33 vents, an anomalously high vent density compared to other low shield volcanoes on the ESRP. Based on the geomorphology of the vents to the south and east of the main Table Butte edifice and un-geotagged photos collected years ago by S. Hughes (*unpublished*), I hypothesized that up to 21 mapped vents from Wetmore et al. (2009) are rootless vents formed from steam explosions on the lava flow (Hughes et al., 1999). I investigated this through fieldwork at the various mapped vent locations. The different ejecta deposits identify primary vents and rootless vents; this includes the size, shape, and distance of the ejecta from the vent opening. One of the main differences is whether the clasts demonstrate evidence of quenching-related fragmentation or are more consistent with welded spatter from a dry eruption (Jones et al., 2018; Zimanowski et al., 1997). I revised the primary vent locations and the number of appropriate events through field observations, including updating the ESRP vents cluster analyses.

Hypothesis Three: Table Butte is a polygenetic volcano.

Most of the low shields of the ESRP are compositionally homogenous, so if Table Butte is composed of a uniform basalt, then the butte is likely to be monogenetic. However, significant changes in mineralogy or geochemistry may indicate the butte indeed formed over multiple events. In this case, it will be essential to consider the distribution and scale of the heterogeneity, as a few low shields on the ESRP, most notably Sixmile Butte, have documented compositional gradients within a continuous eruptive package (Barton, 2020). Thin section and XRF analysis will provide insight into the magma that fed the eruptions, including whether they came from the same magma source. If Table Butte is determined to be a polygenetic volcano, it could indicate elevated probabilities of future events in that area.

1.4- Broader Impacts

Understanding the volcanic history of Table Butte will improve the accuracy of hazard assessments conducted for the ESRP. This study will identify 1) whether the Table Butte eruption involved phreatomagmatism, 2) if more than one event built the Table Butte edifice, and 3) the actual locations and numbers of primary vents. These findings will contribute to improving calculations of local eruption probability. Given that the ESRP is an active monogenetic volcanic field with hundreds of vents and a non-time transgressive spatial pattern, it is entirely possible that the next eruption could impact the Idaho National Lab or one of the towns located on the plain. Successfully creating volcanic hazard maps replies on accurate representation of past eruptions, including the correct types and locations of all observable vents; by correctly mapping and interpreting Table Butte, this project will resolve an open question regarding the vent cluster located there (Fig. 1.3).

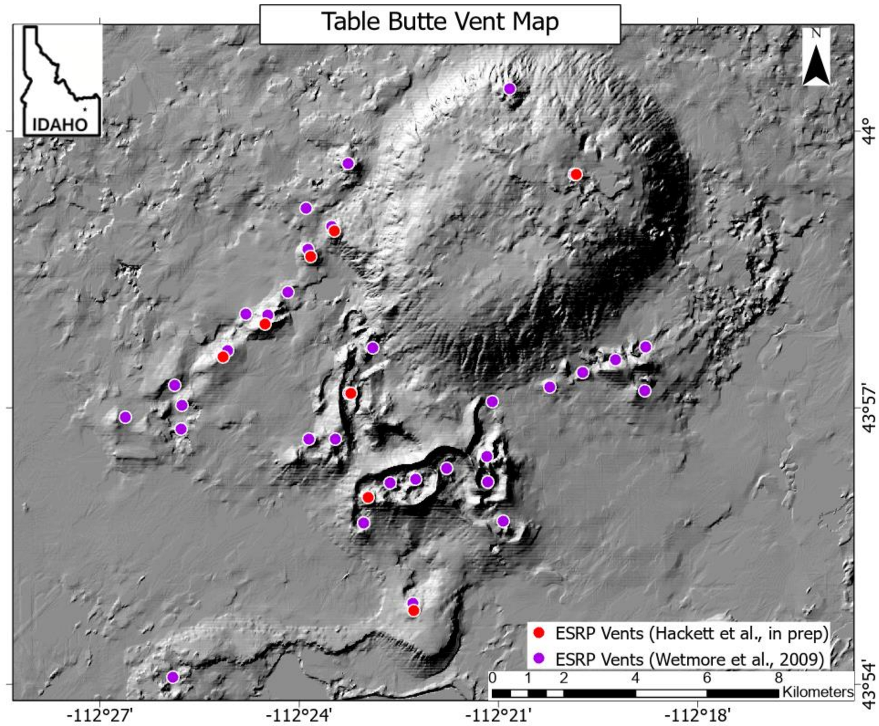

Figure 1.3: Table Buttes vent map using Wetmore et al. (2009) and Hackett et al. (in prep) data

1.5- Organization of the thesis

This thesis follows the "paper" style rather than the traditional "chapter style," so the third chapter is a manuscript intended for submission to a journal. The first chapter of this thesis describes the motivation for this research, including briefly introducing the field area and relevant precursor data. The second chapter, a literature review, provides a more detailed background about the ESRP, Table Butte, and volcanic hazards. Finally, the fourth chapter offers a discussion and conclusion, including recommendations for further work. These bookending chapters (1, 2, 4) represent the explanatory style that will make the work accessible to readers with a general understanding of geology but not necessarily a background in volcanology. Due to the nature of this thesis structure, necessary content from Chapters 1, 2, and 4 then repeats in the standalone journal manuscript, with Chapter 3 adopting a style consistent with the Journal of Volcanology and Geothermal Research or the Bulletin of Volcanology.

Chapter 2 Geologic Background

2.1 Geologic history of the eastern Snake River Plain

The eastern Snake River Plain (ESRP) is an area of active volcanism in Idaho (Fig. 2.1). The Idaho National Laboratory (INL) is currently funding a Probabilistic Volcanic Hazards Assessment (PVHA) following Nuclear Regulatory Commission guidelines to evaluate the potential for future volcanic events affecting their facilities. Understanding the volcanic history of the ESRP is critical to calculating future hazard risk for the plain. In addition, the inclusion of accurate vent and event maps allows researchers to analyze the spatial variability of volcanism over time.

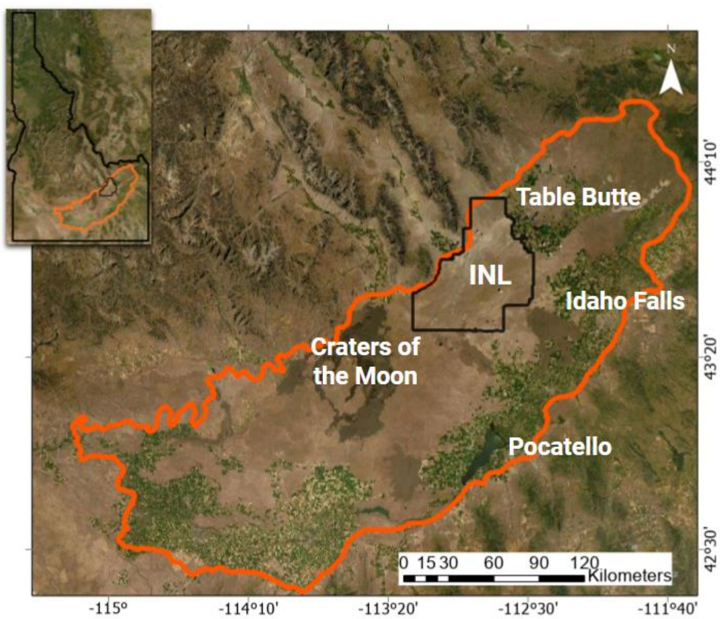

Figure 2.1: The ESRP (orange polygon) covers a wide swath of southeastern Idaho and includes multiple towns/cities, agricultural land, Craters of the Moon National Monument and Preserve, and Idaho National Laboratory (INL; black boundary). Aerial imagery from ArcGIS Pro base map (Esri, 2012).

Approximately ten million years ago, the ESRP started to form due to the passage of the hotspot that lies under Yellowstone National Park today (Pierce et al., 2002; Pierce and Morgan, 1992). Hotspot-related volcanism produced rhyolitic rocks, which generally erupted explosively in large, caldera-forming eruptions, resulting in the emplacement of large-volume ignimbrite tuffs (Branney et al., 2008). The passage of the hotspot also contributed to the formation of what is interpreted to be a sizable mid-crustal gabbroic sill within the lower part of the upper crust (Hughes and McCurry, 2002; Pierce et al., 2002; Rodgers et al., 2002; Wright et al., 2002). The sill is thought to contribute to reduced seismicity in the area and to be the site for mantle basalts to fractionally crystallize into the intermediate and felsic lavas occasionally observed on the ESRP (McQuarrie and Rodgers, 1998). The combined weight of the ESRP lavas, sediment infill, and the mid-crustal sill has caused isostatic down warping of the ESRP (e.g., McQuarrie and Rodgers, 1998; Humphreys et al., 1999; Greeley, R., 1982).

The ESRP is a distributed (i.e., monogenetic) volcanic field. The volcanically active area is widespread and dotted with relatively small volcanoes that only erupt once (e.g., Smith and Nemeth, 2017). Distributed volcanic fields most likely occur in areas of crustal extension (Connor and Conway, 2000; Michon and Merle, 2001; Hughes et al., 2002; LeCorvec et al., 2013a). Most ESRP volcanoes are small shields, although other distributed volcanic fields have dominant features like scoria cones, maars, or tuff cones (Zarazúa-Carbajal and Cruz-Reyna, 2020). The volcanoes in distributed systems begin as dikes in the subsurface, forming fissure eruptions before the erupting material focuses into one or more vents along the original fissure (Connor et al., 2000). The large total volume of lava and its emplacement via many shield volcanoes inspired the term “plains-style” volcanism, a cross between traditional shield and flood basalt systems (Greeley et al., 1982). Lava tubes are standard features in distributed volcanic fields and allow lava to travel greater distances before solidifying, thanks to the insulating properties of the tube (Hughes et al., 1999).

2.1.1 Vents and Events

Volcanic vents are widespread across the ESRP, but there is no definitive map of the surface vent locations. In their recent work on the likelihood of a lava flow entering the INL footprint, Gallant et al. (2018) used a list of vent locations developed by Wetmore et al. (2009) using a combination of published surface maps (Kuntz et al., 1994) and interpolated subsurface vents (Anderson and Liszewski, 1997; Wetmore, 1998) (Fig. 2.2). The Wetmore et al. (2009) dataset, which is still in regular use (ex. Gallant et al. (2018)), includes vent clusters, including those at Table Butte, that were previously flagged as potentially rootless and therefore inappropriate for inclusion as primary vents (Hughes et al., 2002). Ongoing efforts by Hackett et al. (*in prep*) to revise the ESRP vent dataset use published and unpublished maps by Champion and Kuntz (*unpublished*), Garwood et al. (2014), Kuntz (1979), Kuntz et al. (2003), Kuntz (2003), Kuntz et al. (2007), Kuntz et al. (2018), Link and Stanford (1999), Othberg et al. (2012), and Skipp and Kuntz (2009), as well as per-vent confirmation in aerial imagery and topography plus targeted field investigations to investigate ambiguous vent locations. The work in this thesis came from funding as part of the effort to revise the Hackett et al. (*in prep*) vent dataset for the Table Butte area.

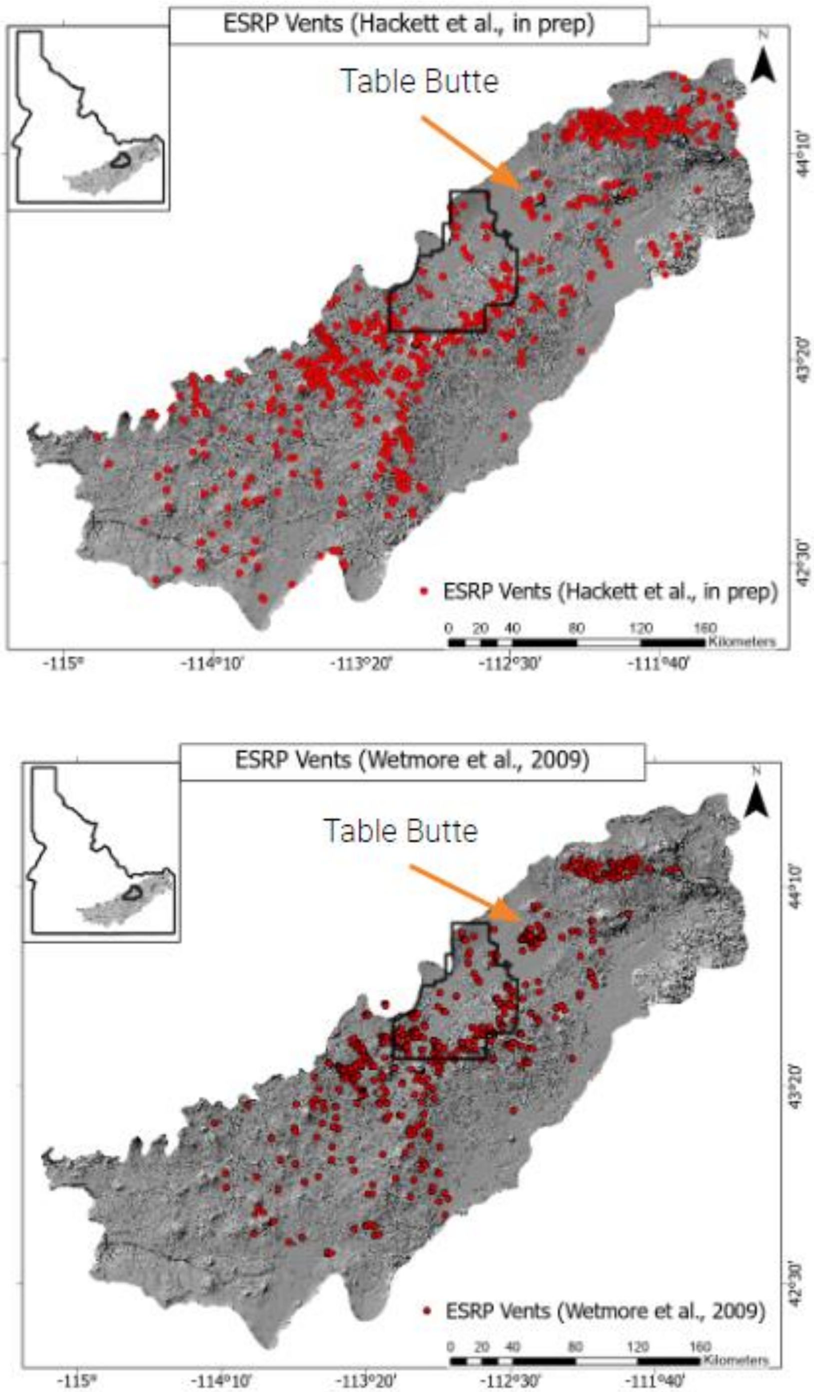

Figure 2.2: Vent location maps for the Hackett et al. (in prep) and Wetmore et al. (2009) data sets. The Hackett et al. (in prep) dataset already includes fewer vents at Table Butte than in the earlier dataset due to re-interpretation of aerial imagery and topographic maps. The Hackett et al. (in prep) dataset revisions do not include field observations.

It is important to clarify that vents and events are not equivalent. A vent is a physical location where magma erupted from the surface. An event, in contrast, refers to an eruptive episode and may involve one or more vents either simultaneously or sequentially over a short period of time. An event is often placed on a map based on the location of one of the contributing vents; there are no standard rules for event location selection, but there is a general preference to use an actual vent location rather than taking the average location of a group of vents (C. Connor, *pers. comm.*). Consider the example of Kings Bowl, a volcanic fissure on the ESRP (Fig. 2.3). Kings Bowl was emplaced during a single volcanic event that occurred ~2 ka (Hughes et al., 2018). There are multiple vents along the Kings Bowl eruptive fissure, marked in Figure 2.3 with white stars. Depending on the rule selected by the mapper, the lone event could be mapped at any of those locations. A hazard map of Kings Bowl based entirely on vent locations would exaggerate the actual threat posed at the site and could create problems when comparing it to older systems where the individual vents may not be as well preserved or exposed. As such, there is value in not only correctly differentiating between primary and rootless vents but also using field relationships and laboratory analyses to interpret the vents within an event framework.

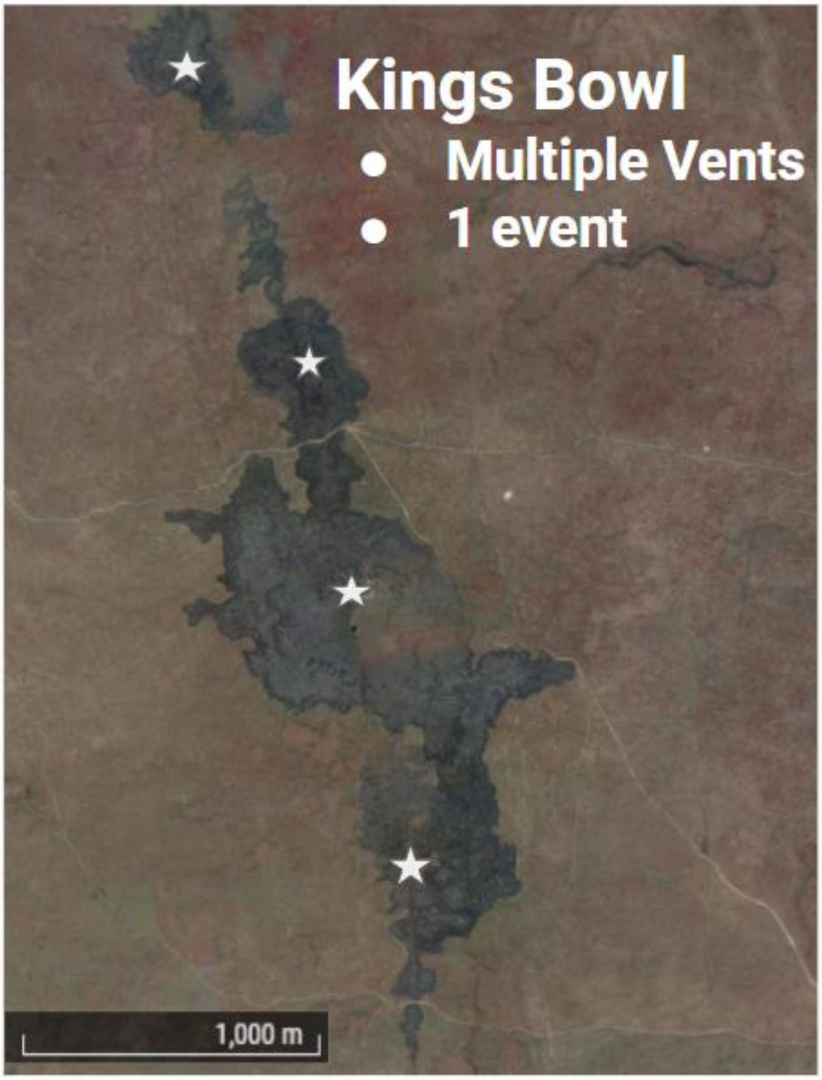

Figure 2.3: Figure showing vent locations along the Kings Bowl fissure on the ESRP. There were multiple vents that contributed to a single eruptive event ~2 ka.

While there is an evolving vent dataset for the ESRP, a similar map of events is not yet available. The Hackett et al. (*in prep*) vents dataset has started to resolve this issue by identifying multiple vents attributed to the same event. Identifying these groupings is challenging and relies on information such as vent orientations, radiometric dating, paleomagnetic data, geochemistry/petrology, and spatial distribution to provide adequate context. This project uses field mapping, petrology, geochemistry, and prior radiometric and paleomagnetic data to establish the number of vents and events represented at Table Butte.

2.1.2 Types of vents

Vents can either be primary or rootless, with only primary vents qualifying for inclusion in the ESRP vent map. Primary vents are sites where lava erupted directly from the subsurface, carried up by the dikes and sills that compose the plumbing system. Rootless vents come from a lava flow surface rather than directly from the plumbing system. For example, they can be spatter cones or hornitos which stem from volatile-rich lava clots bursting from an over-pressured lava tube or craters from steam blasts formed by lava interacting with external water (Jones et al., 2018; Zimanowski et al., 1997). Rootless vents are not related to the underlying plumbing system, so they are not considered appropriate for inclusion with primary vents in the ESRP vent map because they do not help identify the areas of increased eruption probability.

I used field observations to differentiate between primary and rootless vents. Both vent styles could feature spatter or phreatomagmatic blast deposits, so the presence of either is not enough to determine the status of a vent. However, how the deposits are distributed in space and the morphology of the overall units can provide a great deal of insight. For instance, spatter cones and hornitos tend to be very steep-sided, relatively small (one to a few 10s of m across) and perched on a contemporaneous lava surface (Jones et al., 2018; Zimanowski et al., 1997). Steam explosions from a lava flow crossing wet ground can excavate deep craters but are likely to have asymmetric lava accumulation on either side, primarily if the blasts occur at the flow front. Further, the flash cooling and stiffening from the steam explosions will inhibit the same rootless vent from subsequently ejecting primary spatter (Jones et al., 2018). Thus, field observations of vents must consider multiple aspects of morphology and facies identification in order to differentiate between primary and rootless vents.

2.1.3 Plumbing System

Depressurization associated with extension moves the magma from the upper mantle through the lower crust and up through the mid-crustal sill (McQuarrie and Rodgers, 1998). The ESRP magma travels from deep crust and mantle reservoirs (e.g., Leeman et al., 2007; Kuntz et al., 1992). Traveling through different sills and dikes up to the surface creates geochemical differences. Although the geochemical signatures are similar throughout the ESRP, slight differences in volcanic fields and volcanic events inside an area may exist through fractionation (Hughes et al., 2002; McCurry et al., 2008). During transportation to the surface, the basaltic magmas undergo fractional crystallization to reach thermochemical equilibrium of the magma in the dikes and sills (McCurry and Welhan, 2012). The conduits provide passageways for the magma to reach the surface and erupt or stall in the subsurface and solidify (e.g., Hughes et al., 1999; McCurry and Welhan, 2012). As such, the Table Butte lava is anticipated to be a tholeiitic basalt with minimal heterogeneity. Compositional heterogeneity in Table Butte could indicate multiple eruptive events, interaction between two magma bodies, or eruption from a zoned reservoir. Investigation of the types of heterogeneity and their distribution laterally and stratigraphically will aid in the interpretation of the cause.

2.2 Description of the Table Butte Area

2.2.1 Table Butte

Table Butte, located in Clark and Jefferson counties, is of interest because of its considerable number of vents and unusual morphology, coupled with its location just outside of the INL footprint. Table Butte has a circular, flat-topped edifice approximately 6.5 km in diameter and standing 100 m above the surrounding ground. The Table Butte system includes a northeast-southwest lineation of vents referred to as the Needle Butte trend and a pockmarked area called The Breaks located immediately adjacent to the main edifice. The steep sides and a flat top of Table Butte distinguish it from most other volcanoes on the ESRP, which is dominated by low shields. Interpretations of the number of vents located at Table Butte and the area immediately surrounding it range from 33 (Kuntz et al., 1994) to 9 (Hackett et al., *in prep*). However, for twenty years, the cluster of vents at Table Butte has been hypothesized to include rootless vents in The Breaks area (Hughes et al., 2002). Whole-rock K/Ar dating places the age of Table Butte at 173 +/- 36 ka (Champion et al., 1988; Kuntz et al., 1994) while $^{40}Ar/^{39}Ar$ dating yields potential ages of either 392 +/- 10 ka or ~72 ka (Champion et al., *in prep*); the older age was selected as the most likely due to similarities with the nearby Camas Butte and Cedar Butte (Champion, *written communication*, 2021). Paleomagnetic data taken from a few locations on Table Butte is notably different from the majority of the ESRP and suggests that it was emplaced as a singular event during a short-lived magnetic anomaly (Fig. 2.4; Champion et al., *in prep*). The paleomagnetism and radiometric dating samples collected prior to the development of a detailed map for Table Butte and with the assumption that the feature was homogenous; as such, field mapping will reveal whether the data are reasonably applied to the entire system or if the disagreements could be the result of samples collected from material erupted during different events.

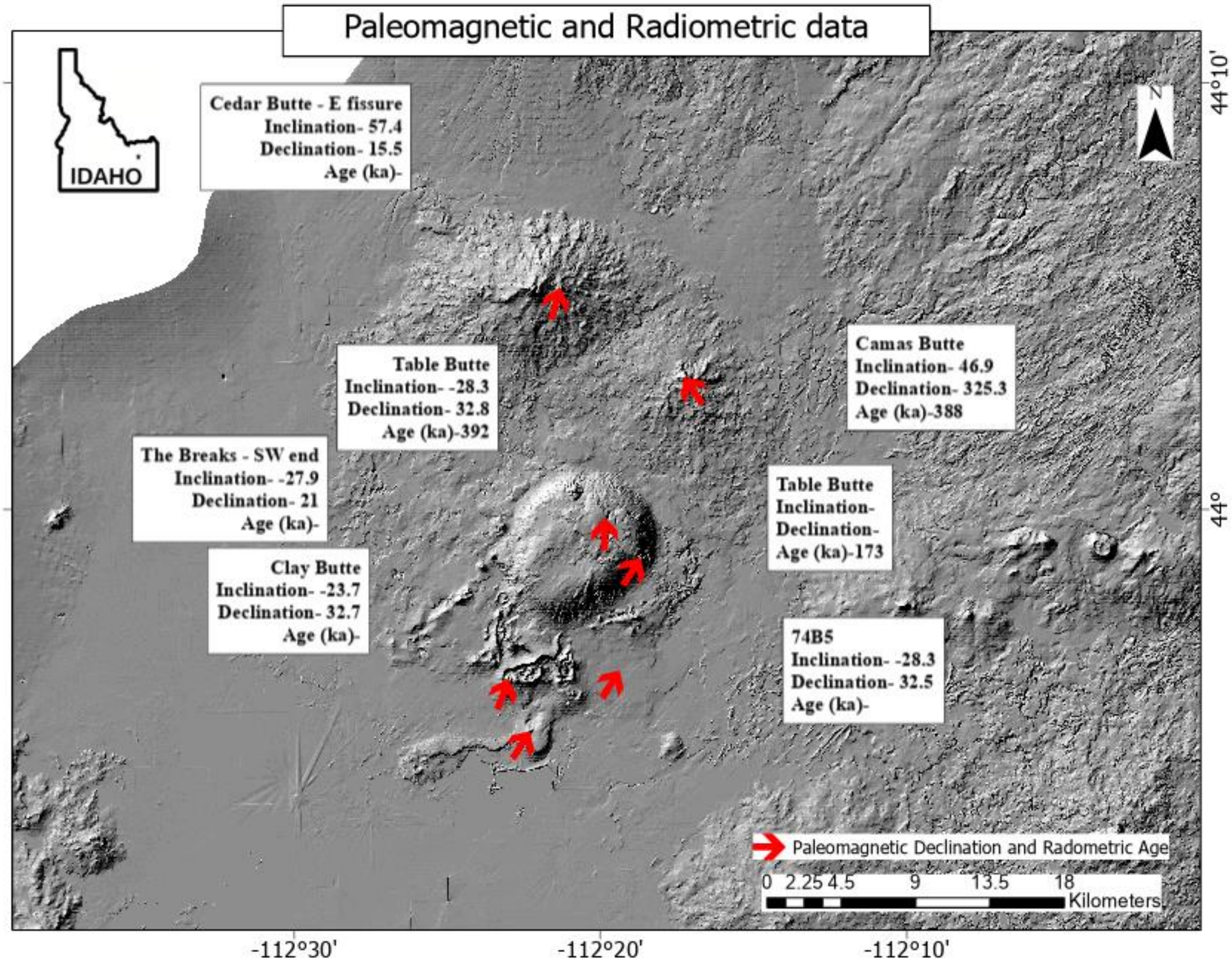

Figure 2.4: Paleomagnetic inclination and declination direction associated with Table Butte and the surrounding area. The base map is a hillshade made from a ten-meter DEM (USGS).

2.2.2 Vents vs. Events

Existing interpretations vary widely on the number of vents at Table Butte (Fig. 2.5) (e.g., Kuntz et al., 1994; Wetmore et al., 2009; Hackett et al., *in prep*). Past vent interpretations of the area used aerial imagery and topography rather than fieldwork, and as a result nearly every crater or pockmark around Table Butte was identified as a vent location. If this interpretation is correct, the Wetmore et al. (2009) data would result in a local vent density of ~0.6 vent/km^2. In contrast, nearby shield volcanoes on the ESRP with similar footprints only have one or two vents

(~0.02-0.06 vents/km^2). However, it is possible that many of the mapped vents at Table Butte are, in fact, rootless (Hughes et al., 2002) and should be removed from the dataset.

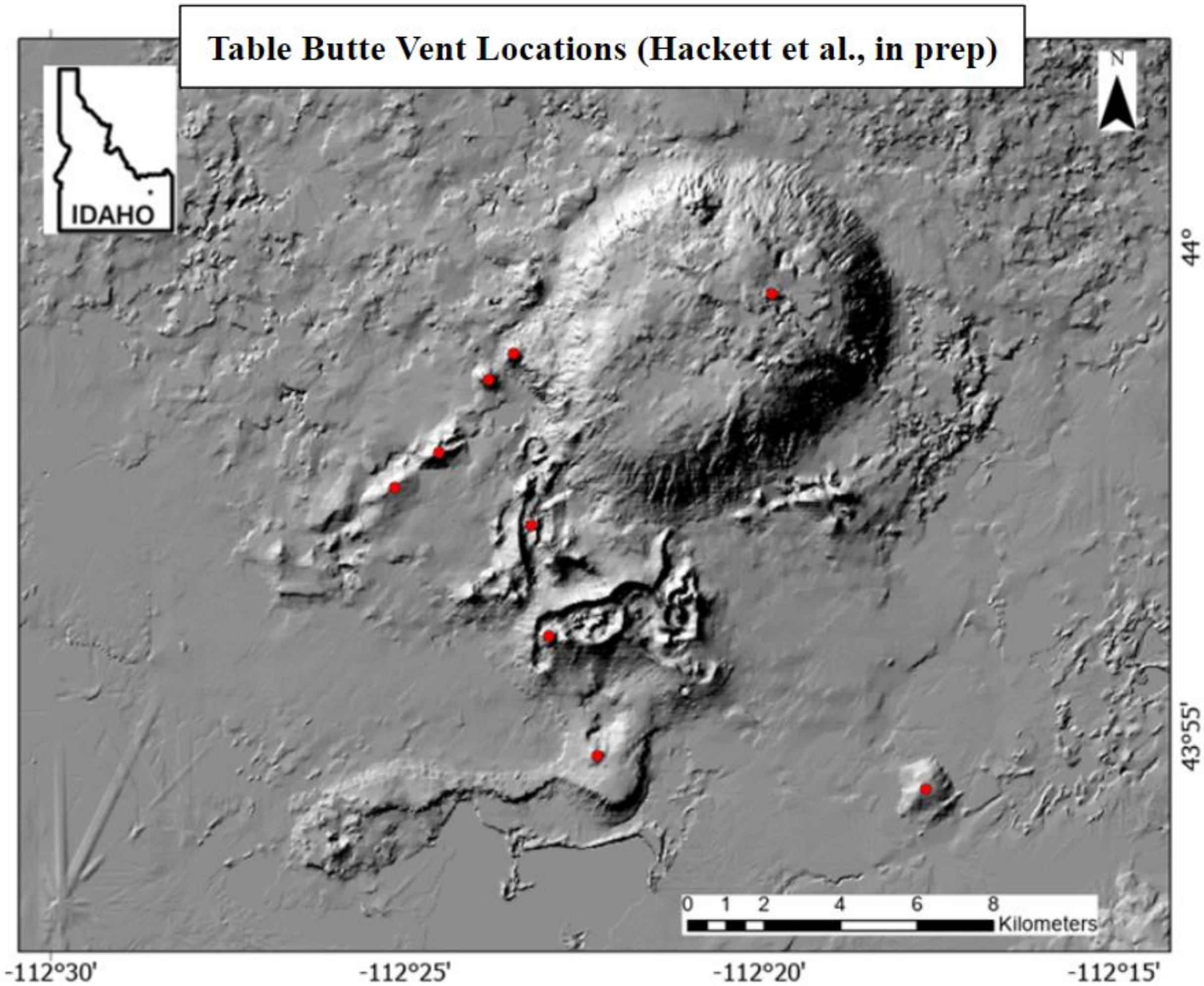

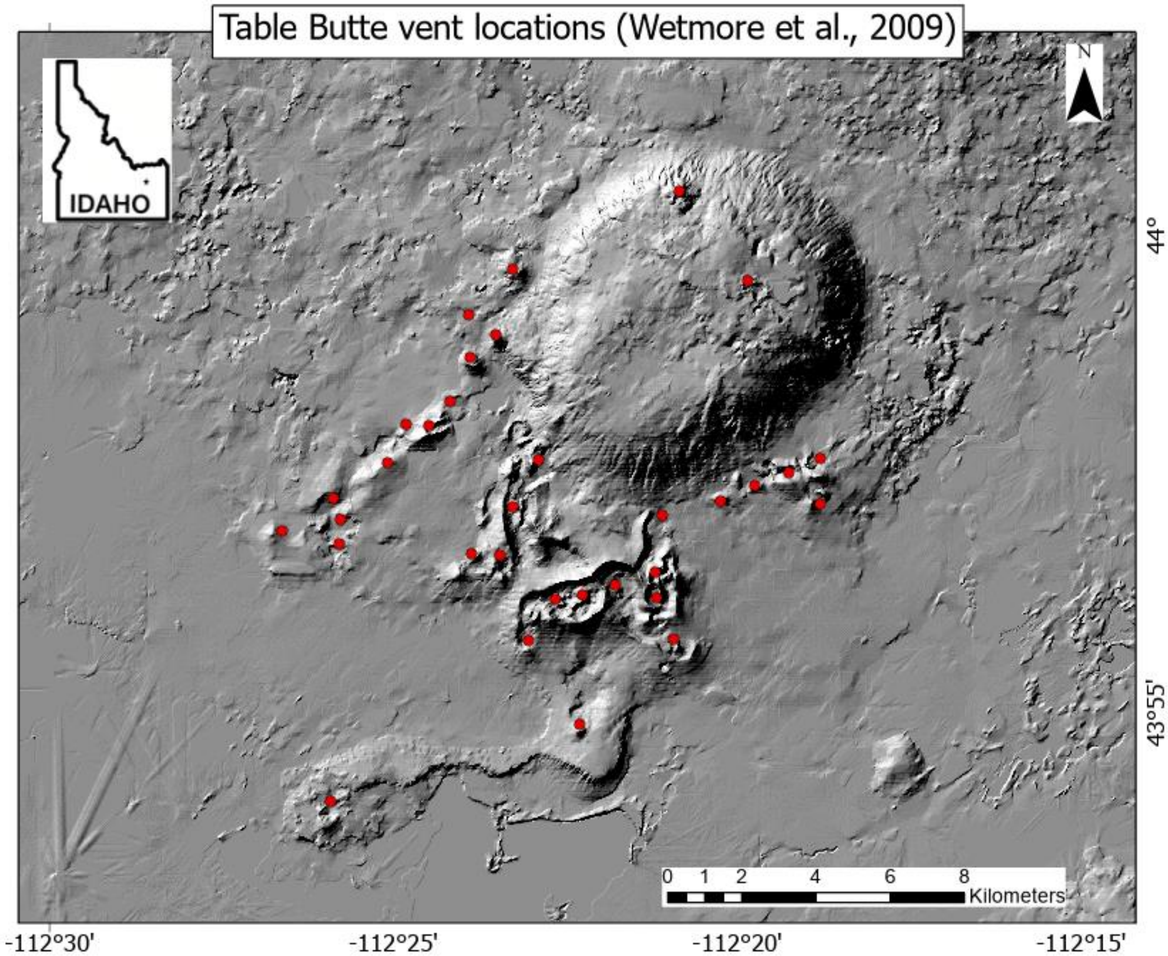

Figure 2.5: Vent locations, marked with red asterisks, at Table Butte from Hackett et al. (in prep) and Wetmore et al. (2009). The two datasets disagree strongly on the number and location of vents at Table Butte, especially in The Breaks. The base map is a hillshade made from a ten-meter DEM (USGS).

2.2.3 Phreatomagmatism

Phreatomagmatism is explosive volcanic activity involving magma and external water undergoing a fuel-coolant interaction. It results in increased fragmentation and explosiveness due to quenching, with the explosivity varying as a function of the relative volumes of water and magma, overburden pressure, etc. (e.g., Morrissey et al., 2000; Zimanowski et al., 1997). Photos taken at Table Butte suggest zones of tephra blast deposits, including lacustrine blocks interbedded with fragmented basalt clasts (S. Hughes, *pers. comm.*). At the same time, other regions of Table Butte only have effusive lava flow deposits. The transition suggests a change from subaqueous to subaerial eruption styles, either associated with vertical growth above the water level or tied to a lateral extent across a dry/wet transition, depending on the spatial distribution of the deposits. One product of water-rock interaction that we looked for at Table Butte is peperite, a sediment and volcanic deposit formed when magma rises through wet soil, creating pepper-like residue (Skilling et al., 2002). Similarly, we looked for palagonite, a rind surrounding volcanic glass that typically appears as a yellowish glass alteration when hot glass touches water (Stroncik and Schmincke, 2001) and poorly vesiculated tephra in blast deposits (poorly sorted, possibly complex grading/bedding), including clasts of displaced lacustrine sediment or river cobbles. Photographic evidence from an old field trip indicates that there are at least some areas of phreatomagmatism at Table Butte, but their locations and extents were unclear from the preliminary data.

2.2.4 Regional paleolakes and groundwater

There is geologic evidence of lakes in the Table Butte area from 17 ka to the present (e.g., Gianniny et al., 2002). Although there is no documented evidence of lakes at Table Butte around 392 ka, the recurrence of surface water in the area and the unusually shallow groundwater table suggest that the site may have been adequately wet to induce phreatomagmatism at the time of the eruption(s). The Mud Lake basin has held multiple small lakes, both historically ephemeral and currently filled in sedimentary deposits (Stearns et al., 1939). These lakes primarily formed due to groundwater discharge close to, or below, the water table, with some drainage runoff influencing lake level and development (Spinazola, 1994). $\delta^{18}O$ levels measured from ocean sediments signify a warm climate around 400 ka, suggesting that surface water was likely to have existed in the Table Butte area based on extrapolation climate-water correlations from recovered lake core (Lisiecki and Raymo, 2005). Even in the absence of surface water, the modern aquifer near Table Butte is remarkably shallow for the ESRP: it is currently less than 10 m below the ground surface, thanks to a shallow aquitard formed by a paleosol (Fig. 2.6) (Spinazola, 1994).

Although most volcanoes on the ESRP do not have evidence of phreatomagmatism, a few, such as Kings Bowl and Menan Buttes, demonstrate profound effects from water-magma or water-rock interaction (Hughes et al., 2018). Menan Butte's tuff cones and rings occurred in an area of extensive surface and shallow groundwater (Spinazola, 1994). In contrast, Kings Bowl, a phreatic blast pit in a lava lake, and Split Butte, a tuff cone, are located in the ESRP without surface water or shallow groundwater (Hughes et al., 2018).

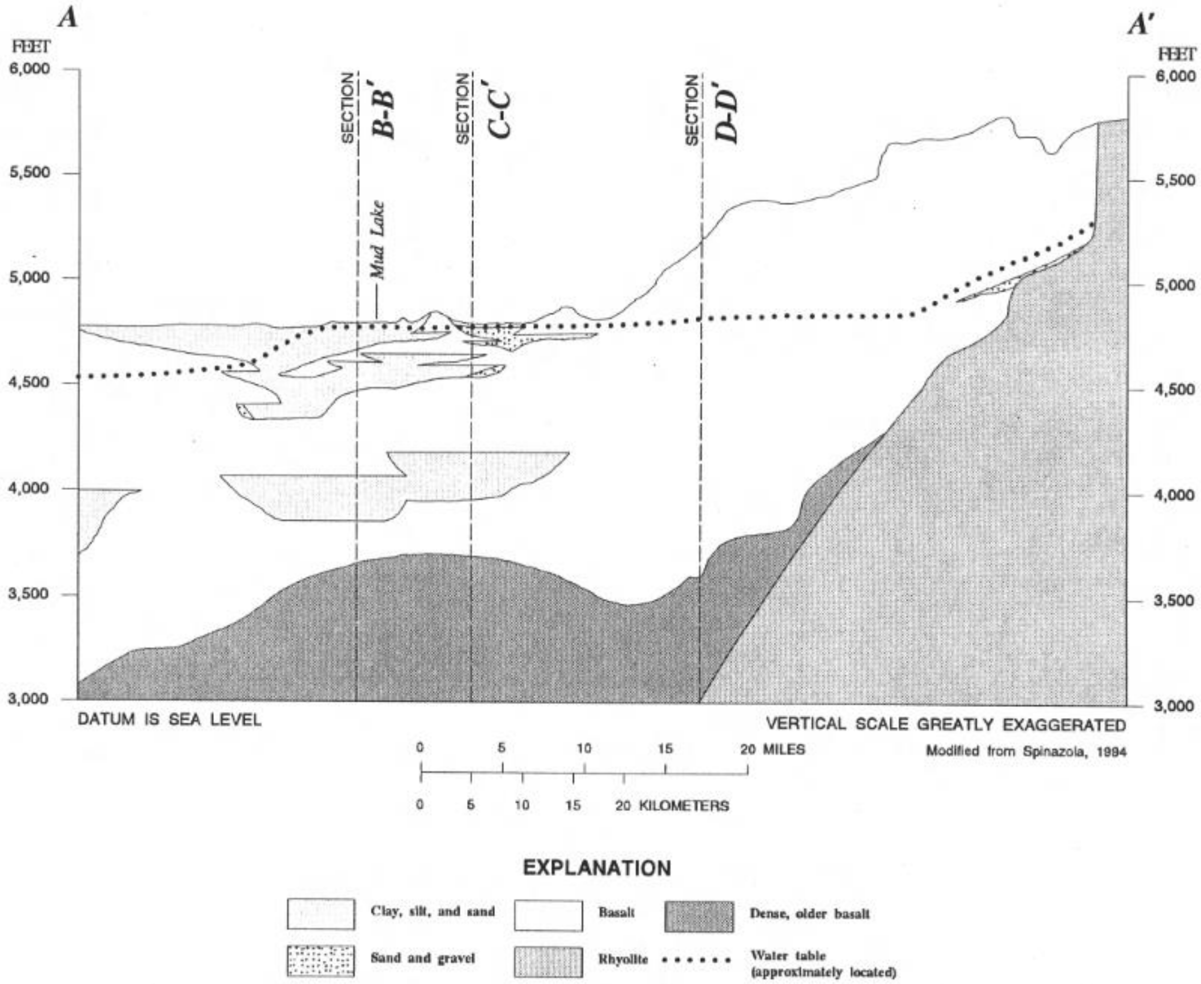

Figure 2.6: ESRP aquifer level compared to Mud Lake and Table Butte. Table Butte in the figure sits between sections B and C as the hill in the image is close to C. Figure 7 from Spinazola (1994).

2.2.5 Sediments

Additional features associated with Table Butte are linear and hairpin parabolic dunes, alluvial fans, and pluvial lakes (Forman and Pierson, 2003). While the focus of this work does not include the study of sedimentary units, they are noteworthy for their influence on the study area. In particular, the sand dunes bury outcrops and create barriers for vehicles, and the pluvial sediments provide evidence of past hydrologic conditions related to phreatomagmatism.

2.3 Statistical Analysis

2.3.1 Cluster Analysis

Cluster analysis is a statistical method that places different variables together depending on how alike they are. One such cluster analysis called multivariate clustering comes from statistical analysis of different correlating information and plots them in a cluster depending on similarities. For the research we did the multivariate cluster analysis will combine both the thin section and XRF data to provide evidence for the four rock units' breakdowns. Multiple tools make up the multivariate cluster analysis. First, the Pseudo F statistic provides an overview analysis of the data and provides an elbow plot where the number of clusters included in the analysis comes from the point where the line bends drastically minimizing error. Then the multivariate cluster tool uses the number of clusters from the elbow plot and places comparable items into a singular category. Thus, showing the clusters of each data points similarities or showing that there are no clusters in the dataset (Jain, 2009).

2.3.2 Kernel Density Estimations

Kernel density estimations (KDE) measure how dense features are in a spatial capacity of a dataset (Silverman, 1986). KDE provides the necessary means to provide the density analysis for vents and events within a volcanic field. Hazards analysis uses KDE to provide insight into the repetition of past hazards. Specifically for volcanic hazards, it provides a view into where the most eruptions take place inside of a volcanic field (Gallant et al., 2018). Using KDE for this research will update the current KDE done by Gallant et al., (2018) with the update to Table Buttes number of vents.

2.4 Hazards Analysis

Given that the ESRP is an active distributed volcanic field with hundreds of vents and a non-time transgressive spatial pattern, the next eruption could impact the Idaho National Lab (INL) or the towns on the plain. Battelle Energy Alliance (BEA) and INL are actively conducting a Probabilistic Volcanic Hazard Assessment (PVHA) following the Nuclear Regulatory Commission's Senior Seismic Hazard Analysis Committee (SSHAC) Level 3 guidelines; work in this thesis was supported by funding from a New Data Collection and Analysis (NDCA) agreement awarded by the PVHA with the purpose of improving geological maps of the area by identifying the numbers and locations of vents and events at Table Butte.

Volcanic hazards on the ESRP include lava flows, explosive eruptions, ballistic projectiles, finer tephra, and deadly gas release. The specific hazards posed by any one eruptive event will vary depending on the magma composition and eruptive environment. Preliminary evidence from satellite imagery, topography, and old photos indicate that Table Butte is among the few volcanoes of the ESRP to have experienced significant explosivity in addition to effusively. Thus, further investigations of Table Butte's eruptive styles and the distribution of products associated with the volcano is necessary to better constrain future volcanic hazards.

A common way to measure vent distribution across a distributed volcanic field is to use kernel density estimation (KDE) (e.g., Connor et al., 2019). The KDE for the ESRP with Hackett et al. (*in prep*) data set shows the central cluster of vents located around Craters of the Moon and Spencer Highpoint (Fig. 2.7). The Wetmore et al. (2009) dataset used by Gallant et al. (2018) in their recent assessment of volcanic risk to INL includes many vents at Table Butte, thereby driving up the local KDE and interpreted probability of a future event in the area. Figure 2.7

illustrates that the number of vents mapped at Table Butte has a meaningful impact on whether the area represents a zone of elevated risk. The Hackett et al. (*in prep*) vent dataset has far fewer vents at Table Butte and therefore anticipates and lower KDE and future probability of an eruption. Finalizing and clarifying the vent mapping with fieldwork for Hackett et al. (*in prep*) will enhance the KDE and provide a precise density characterization for the ESRP. The ESRP is home to multiple cities, farmland, ranch land, and infrastructures, including INL. The research done for this thesis to understand the recurrence rate, spatial distribution, and potential hazards at Table Butte will improve the KDE and probabilistic volcanic hazard assessment for this part of the ESRP. Ultimately, the study of ESRP volcanic hazards and subsequent work to mitigate risk during future events are critical for the future of Idaho.

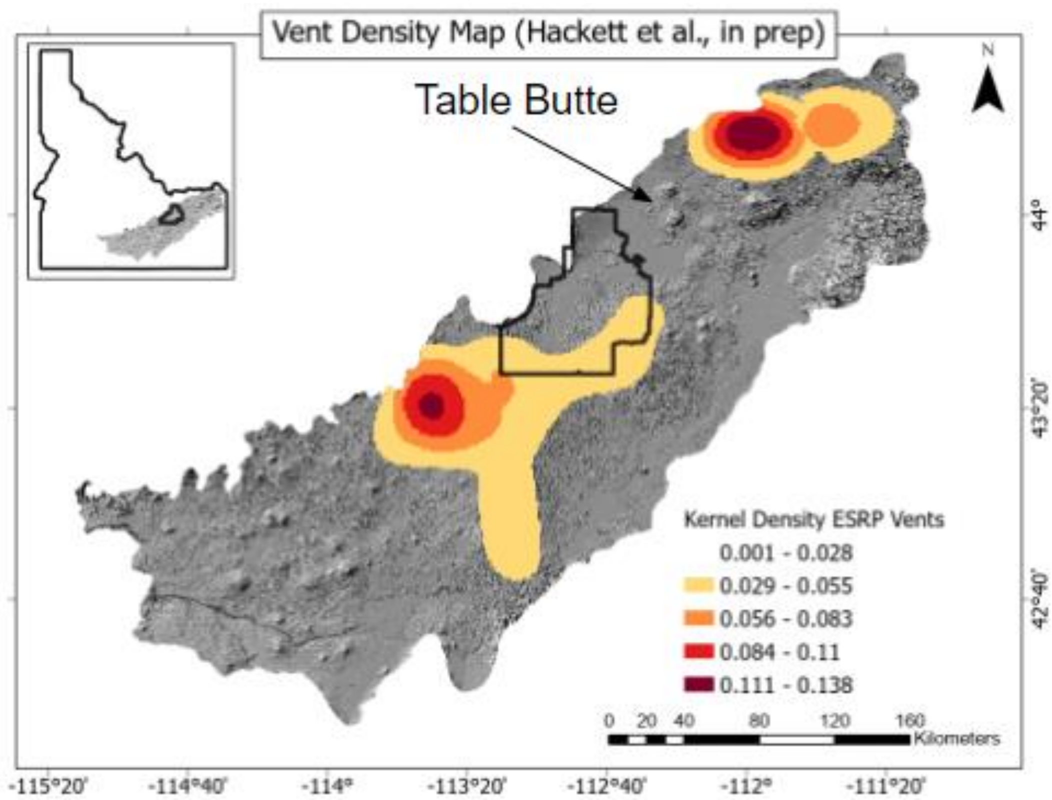

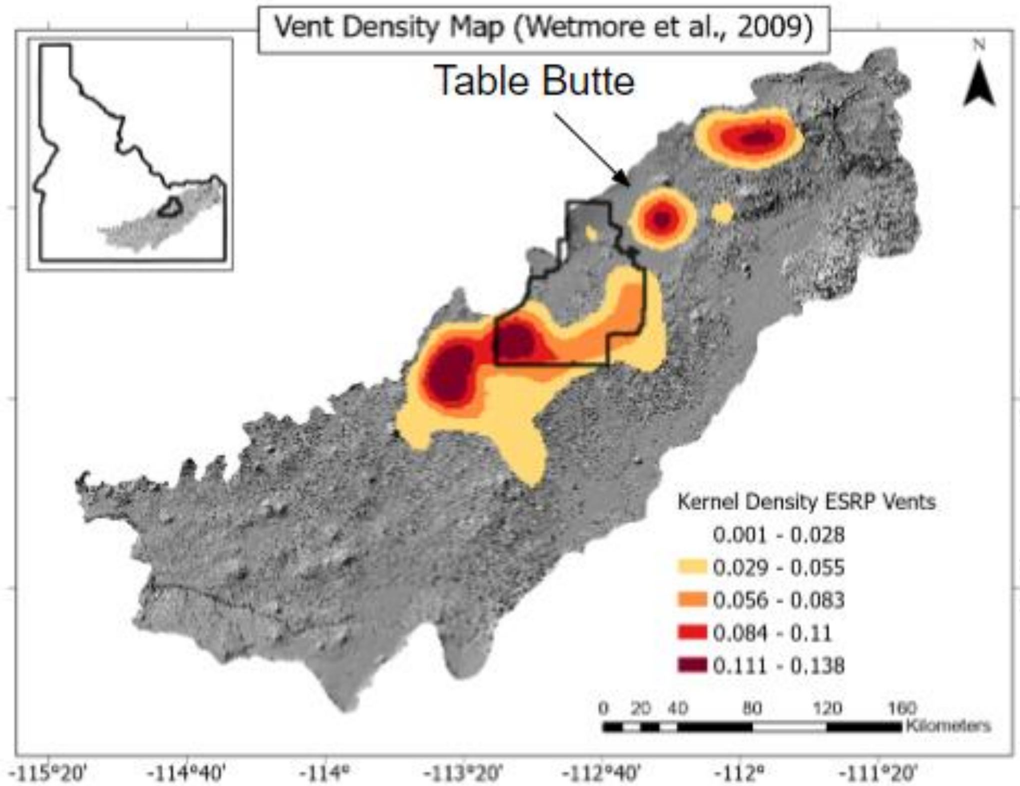

Figure 2.7: Kernel density of the ESRP vent distribution using data from Hackett et al. (in prep) and Wetmore et al. (2009) on top of hillshade image created from a ten-meter DEM (USGS) dataset.

Chapter 3: Journal Submission

3.1 Introduction

Table Butte, an olivine tholeiite shield volcano on Idaho's eastern Snake River Plain (ESRP), has long been suspected of having incorrectly mapped vents (Hughes et al., 2002). With over 30 mapped vents on and immediately around Table Butte, the location represents a notable area of elevated vent density on the ESRP (e.g., Kuntz et al., 1994; Wetmore, 2009). Table Butte has steep sides and a flat top, an unusual morphology for the ESRP, which is dominated by low shield volcanoes plus the occasional done, scoria cone, or tuff cone (Fig. 3.1). In addition, the area immediately south and west of the main edifice is pocked by a series of overlapping craters, also atypical of the volcanic field. The anomalously high vent density, along with the unusual morphologies present, have led past researchers to speculate that some of the mapped vents are rootless (Hughes et al., 2002). If this is true, it creates meaningful errors in probabilistic hazard assessments of the area, such as the one conducted by Gallant et al. (2018). Volcanic hazards analysis relies on complete geologic maps of volcanic fields to understand past and future events (e.g., Condit and Connor, 1996). As such, this work uses fieldwork, petrology, and geochemistry to investigate Table Butte and offer the first updated detailed geologic map and history specific to that area. The updated geologic map consists of the minimum extent bedrock and includes minimal extrapolation to areas inaccessible due to property permissions or burial by modern sediment.

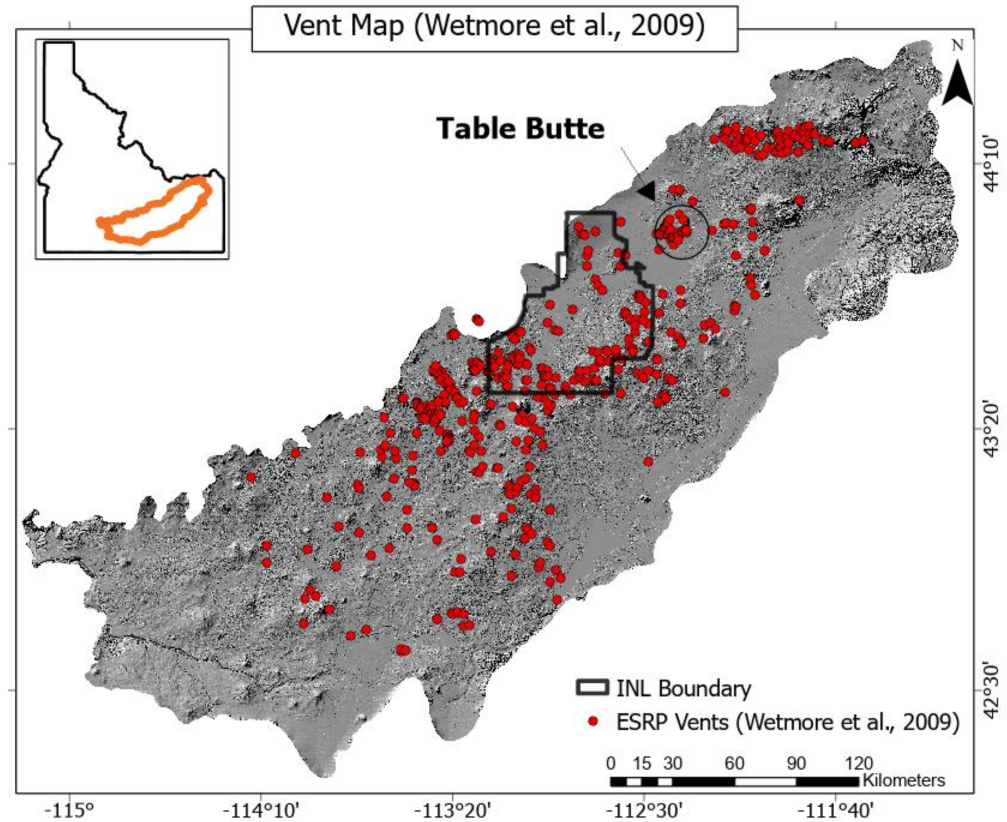

Figure 3.1: Regional setting of the vent locations from Wetmore et al. (2009) overlaying a hillshade from a 10 m/pixel DEM (USGS). Idaho National Laboratory (INL) is a key feature concerning hazard assessments (e.g., Gallant et al., 2018). However, the ESRP also contains multiple small to medium-sized cities and extensive agricultural areas.

3.2 Regional setting

The ESRP, spanning 350 km x 100 km in southeast Idaho, is bordered by the Basin and Range Province to the north and south. The ESRP formation started with the Yellowstone hotspot's passage from 10 Ma to 2.1 Ma (e.g., Branney, et al., 2008). Following the caldera-forming rhyolitic eruptions from the hotspot, the area has experienced an extended period of distributed volcanism dominated by olivine tholeiite lava (Hughes et al., 1999). A mid-crustal gabbroic sill is inferred to have developed from mafic lavas stalling in the crust due to buoyancy (McQuarrie and Rodger, 1998); the sill is sufficiently massive that it is thought to cause isostatic down-warping of the crust (e.g., Greeley, R., 1982; Humphreys et al., 1999; McCurry and Rodgers, 2009). The mid-crustal sill is considered the source of rhyolite domes erupted onto the ESRP, as primitive magmas trapped there undergo extreme fractional crystallization to produce rhyolitic melt (Branney et al., 2008). In contrast, other primitive magmas pass through the mid-crustal sill, experiencing minimal change from their upper-mantle form and erupting as tholeiitic basalt (e.g., Branney et al., 2008; McCurry et al., 2008; McQuarrie and Rodger, 1998).

The ESRP is the type of location for plains-style volcanism. Greeley (1982) described the region as a hybrid between shield and flood volcanism, resulting in a thick stack of small shield volcanoes and fissure-fed lava flows. The Kimama deep core hole revealed a more than a mile thick basalt sequence, though the total depth varies across the field (Potter et al., 2019; Twining and Bartholomay, 2011).

There are currently over 600 surface vents mapped on the ESRP (Wetmore et al., 2009; Gallant et al., 2018). While most mapped vents are monogenetic basaltic shields, the plain also includes at least one polygenetic zone along a rift (the Great Rift at Craters of the Moon), various intermediate lava compositions, several rhyolitic domes and cryptodomes, and a few scoria and tuff cones. Surface vents are irregularly distributed in space, with clusters mapped in the Spencer-High Point area near the current Yellowstone hotspot location, along the Great Rift at Craters of the Moon, around Table Butte, and along the plain's Axial Volcanic Zone (AVZ) (Fig. 3.2). Rhyolite domes are located along the AVZ, while most scoria cones are in the Craters of the Moon and Spencer-High Point areas. Tuff cones are infrequent and occur in areas of long-term surface water, such as Menan Buttes, and regions of relatively deep groundwater, like at Split Butte; there is no clear pattern to their distribution across the ESRP.

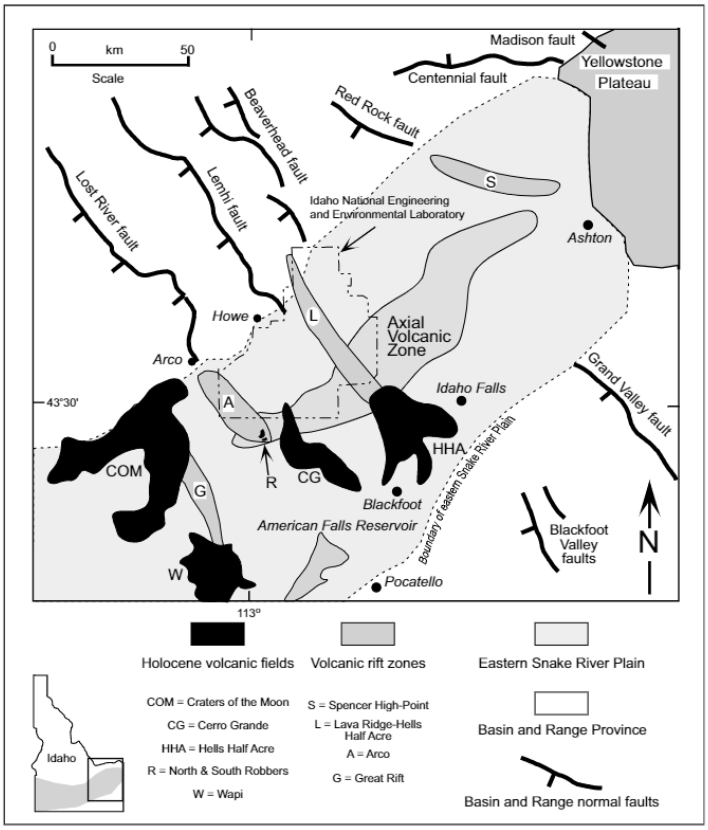

Figure 3.2: Schematic map of the ESRP. Figure 1 from Hackett and Smith (2002).

Table Butte, an ESRP volcano with unusual morphology and apparent vent density, is close to Idaho National Laboratory (INL) and the city of Mud Lake. The Table Butte system spans 10 km x 13 km, including Needle Butte, Clay Butte, and The Breaks (Fig. 3.3). Although the majority of ESPR tholeiitic volcanoes are low shields, the main edifice of Table Butte has steep sides and a flat top, and the surrounding units include an anomalously high number of craters. Table Butte resides in a subbasin of the ESRP and has a history of shallow lakes, including multiple dry lake beds and modern-day Mud Lake directly to the south (Gianniny et al., 2002). Surface water on the ESRP is uncommon outside of the Snake River, making the lakes and marshes by Table Butte noteworthy.

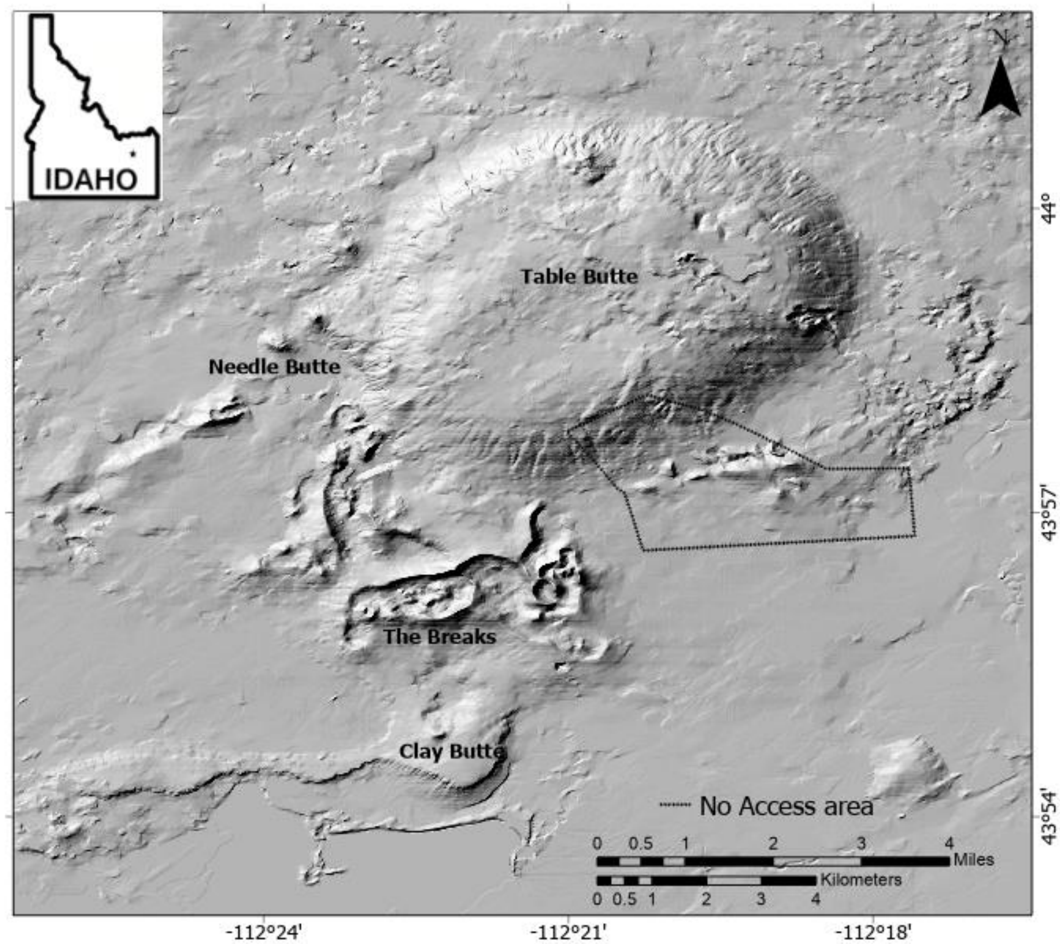

Figure 3.3: Hillshade of the Table Butte area displaying the unusual morphologies present: the flat top and steep sides of the main Table Butte edifice and the overlapping craters of The Breaks. Most tholeiitic ESRP volcanoes are low shields or lava flow fields.

3.3 Material and methods

3.3.1 Imagery and map analyses

We used DEMs, aerial imagery, and multiple maps in this study: a 1:100,000 map of INL (Kuntz et al., 1994), a 1:50,000 map of Circular Butte (Kuntz, *unpublished*), the 10 m DEM for the ESRP (U.S. Geological Survey, 3D Elevation Program 10-Meter Resolution Digital Elevation Model), National Agriculture Imagery Program (NAIP) and ArcGIS Pro base maps, and the vent dataset compiled by Wetmore (2009) and used most recently by Gallant et al.

(2018). In addition, we used a version of the vent dataset currently in development by Hackett et al. (*in prep*). We used the aerial imagery and topographic data to review the vents in the Wetmore (2009) and Hackett et al. (*in prep*) datasets and create a targeted field plan to evaluate whether they were primary or rootless nature and establish the overall geologic history of Table Butte.

We also benefitted from limited unpublished geochemical analyses and field photos (Hughes, *unpublished*) and paleomagnetic and $^{40}Ar/^{39}Ar$ age data (Fig. 3.4) (Champion et al., *in prep*). None of these datasets offer comprehensive coverage of the Table Butte system, but they provide helpful context. The geochemical data are consistent with olivine tholeiites (Hughes, *unpublished*), the most common rock type on the ESRP. The sole radiometric age from the Table Butte system, taken from a sample from the top of the main edifice (Champion et al., *in prep*), suggests an age of ~400 ka. The multiple paleomagnetic analyses show a consistent and unusual orientation indicative of a short-lived magnetic incursion (Champion et al., *in prep*).

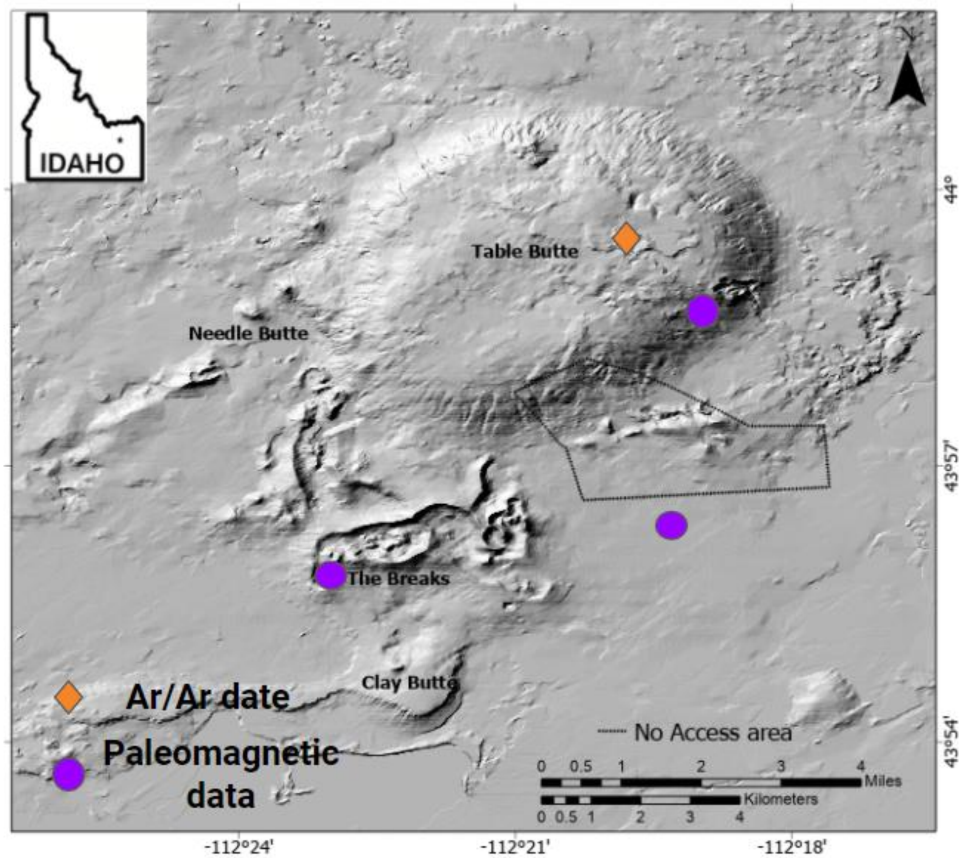

Figure 3.4: Table Butte map shows the different samples sites including one Ar/Ar date and three paleomagnetic analyses. Hillshade imagery built from a DEM of Table butte created the base map (USGS).

3.3.2 Fieldwork

We collected multiple samples from each of the subzones of the field area: Needle Butte trend, north-south trending Breaks, east-west trending Breaks, and the main Table Butte edifice (Fig. 3.5; table 3.1). Field observations focused on outcrop textures, such as spatter-fed lava and phreatomagmatic ejecta. Samples were tentatively categorized into four units in the field based on hand-sample observations of crystal assemblages.

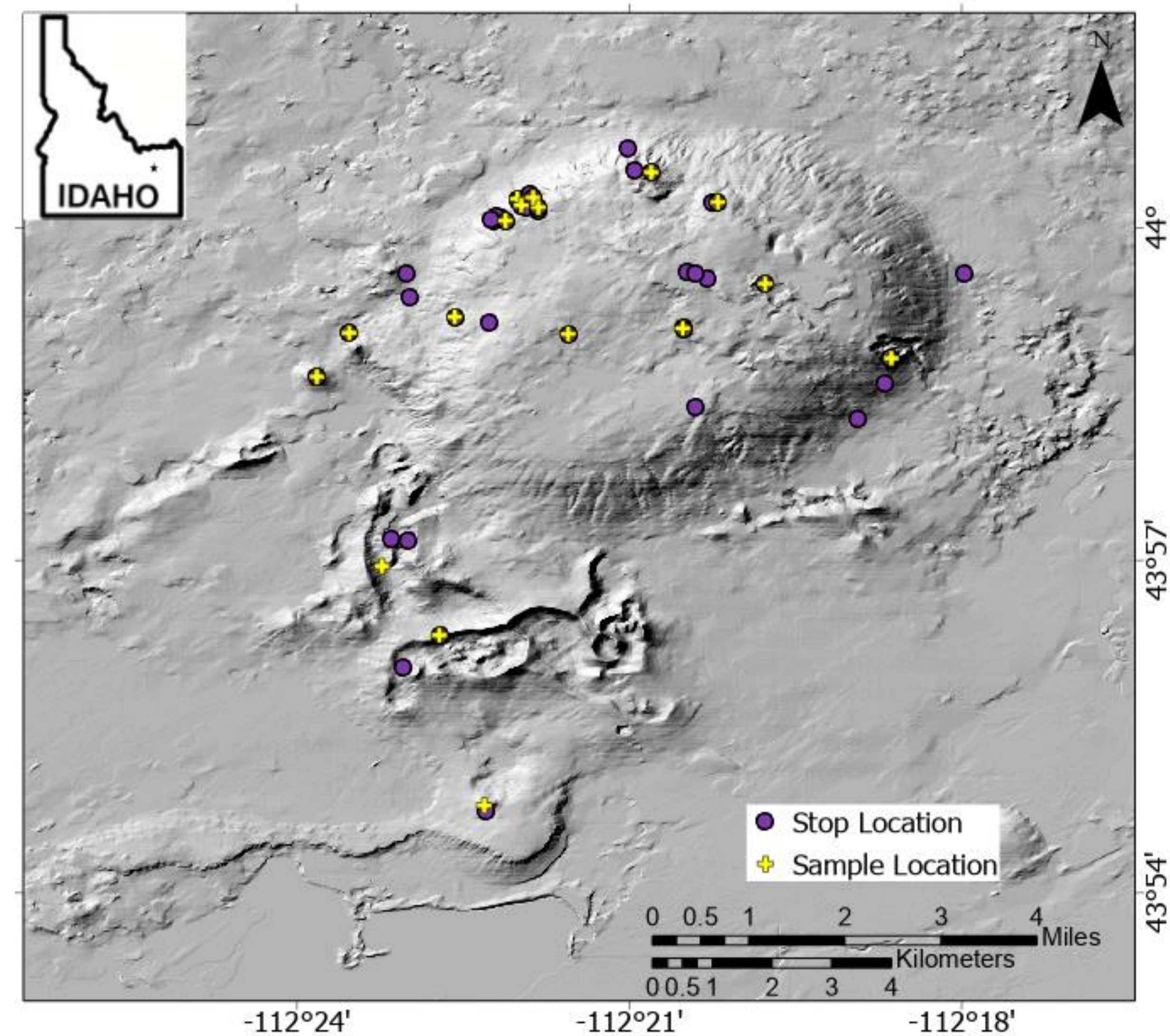

Figure 3.5: Stop and Sample locations from fieldwork.

Table 3.1: Locations of samples and field observations. Latitude and are reported in NAD 1983 UTM 12N.

Stop ID	***Sample ID***	***Longitude***	***Latitude***
1	*CB1*	*43.91239585*	*-112.3715859*
2	*BR-1*	*43.93896958*	*-112.3786236*
3		*43.93409064*	*-112.3839932*
4	*TB1*	*43.97681882*	*-112.311794*
5	*TB21*	*43.980652*	*-112.3108827*
6		*43.97326723*	*-112.3401654*
7	*TB2*	*43.99175833*	*-112.3296767*
8	*TB3*	*44.00831093*	*-112.3693123*
9	*NB1*	*43.98432665*	*-112.392189*
10		*44.0121404*	*-112.3502032*
11		*44.01209031*	*-112.3502254*
12	*TB4*	*44.00875638*	*-112.3493493*
13	*TB5*	*44.00847448*	*-112.3467707*
15		*43.99252743*	*-112.3382843*
16		*43.99325681*	*-112.3401077*
17		*43.99353543*	*-112.3415217*
18	*TB6*	*44.00103122*	*-112.3704024*
19	*TB7*	*44.0019292*	*-112.3702177*
20	*TB9*	*44.00168083*	*-112.3693925*
21	*TB8*	*44.00143394*	*-112.3709091*
22	*TB10*	*44.0012171*	*-112.3686861*
23	*TB11*	*43.99324465*	*-112.3834558*
24	*NB3*	*43.99323889*	*-112.3836139*
25	*NB2*	*43.97778889*	*-112.397*
26	*TB13*	*44.00420913*	*-112.3668662*
27	*TB14*	*44.00352067*	*-112.3663057*

28	*TB15*	*44.00314444*	*-112.3654389*
29a	*TB16*	*44.002675*	*-112.3637778*
29b	*TB17*	*44.00323611*	*-112.3637361*
30a	*TB18*	*44.005106*	*-112.36504*
30b	*TB19*	*44.00471389*	*-112.36455*
31	*TB20*	*44.00401111*	*-112.3367917*
32		*43.93409167*	*-112.3839944*
33		*43.93896944*	*-112.378625*
34		*43.99175833*	*-112.329675*
35		*43.99333333*	*-112.2997222*
36	*TB22*	*43.98962242*	*-112.3830486*
37	*TB23*	*43.9867761*	*-112.3763073*
38	*TB24*	*43.98597108*	*-112.3710763*
39	*TB25*	*43.98418732*	*-112.3592692*
40	*TB26*	*43.98506942*	*-112.3420543*
41		*43.97152411*	*-112.3158856*
42		*43.98417778*	*-112.3592722*
43		*43.98499722*	*-112.34205*
44	*BR-3*	*43.9533404*	*-112.3858928*
45	*BR-2*	*43.95307616*	*-112.3833826*
46	*TB-27*	*43.990742*	*-112.294169*
47	*TB-28*	*43.981381*	*-112.335548*
48	*BR-4*	*43.957412*	*-112.378743*
49	*BR-5*	*43.959083*	*-112.378008*
50	*TB-21-SKN1*	*44.00525*	*-112.362772*
51	*TB-21-SKN2*	*44.003636*	*-112.36625*
52	*TB-21-SKN3*	*44.005047*	*-112.367347*

3.3.3 Thin-section analysis

A subset of the samples underwent petrographic point count analysis. Thin sections were single polished and 1" x 2"; each was analyzed via 1000 points counted on a petrographic microscope with a standard point counting stage. Based on a pre-analysis review of the slides, the point counting categories used were plagioclase, olivine, vesicle/secondary infill, and matrix. Results were re-normalized to remove void space and secondary infill from eolian dust and caliche (Van Der Plas and Tobi, 1965). The point counts were used to confirm and refine field-based identification of the rock units.

3.3.4 X-ray Fluorescence

Samples that underwent petrographic point counting were also analyzed by whole-rock XRF analysis for major element oxides (%) and minor elements (ppm). The samples were trimmed to minimize the presence of secondary infill, crushed, agitated in a bath of 100 ml of 33% hydrochloric acid and 400 ml of deionized water for 10 minutes to remove additional possible caliche, dried, and powdered using a grinder till with a tungsten carbide puck. The XRF analyses were conducted by the analytical geochemistry laboratory at Brigham Young University following standard XRF techniques (Dailey, 2016).

3.3.5 Cluster Analysis

To compensate for the challenges in differentiating between low-crystallinity basaltic lavas, we used multivariate clustering of the mineral modes and major and minor element data to determine rock unit classifications. This included using an elbow plot (pseudo-F statistic) to confirm that there were four differentiable map units.

3.3.6 Kernel Density Estimations

Kernel density estimations (KDE) measure how dense features are in a spatial capacity of a dataset (Silverman, 1986). KDE provides the necessary means to provide the density analysis for vents and events within a volcanic field. Hazards analysis uses KDE to provide insight into the repetition of past hazards. Specifically for volcanic hazards, it provides a view into where the most eruptions take place inside of a volcanic field (Gallant et al., 2018). Using KDE for this research will replace the most-recent KDE done by Gallant et al., (2018) with the update to Table Buttes number of vents.

3.4 Results

3.4.1 Outcrop morphologies and spatial relationships

Each of the Table Butte area subzones had distinctive textures observable in aerial imagery and in outcrop. The Breaks, subdivided into east-west and north-south trending sections, are characterized by alternating layers of phreatomagmatic ejecta and spatter/spatter-fed lava, with layers sloping outward away from the local axis. Phreatomagmatic layers have well-sintered, poorly sorted, dense, glassy clasts of basalt with frequent lacustrine sediment clasts ranging in size from sand grains to half-meter blocks and dense basalt rip-up clasts up to a meter across (Fig. 3.6). The spatter-dominated layers include numerous dense basalt clasts, regularly 10-15 cm in diameter. Morphologically, the largest difference between the two subzones of The Breaks is that the topography is less pronounced along the north-south trend, suggesting that it may be somewhat older and more weathered than the east-west trending portion of The Breaks.

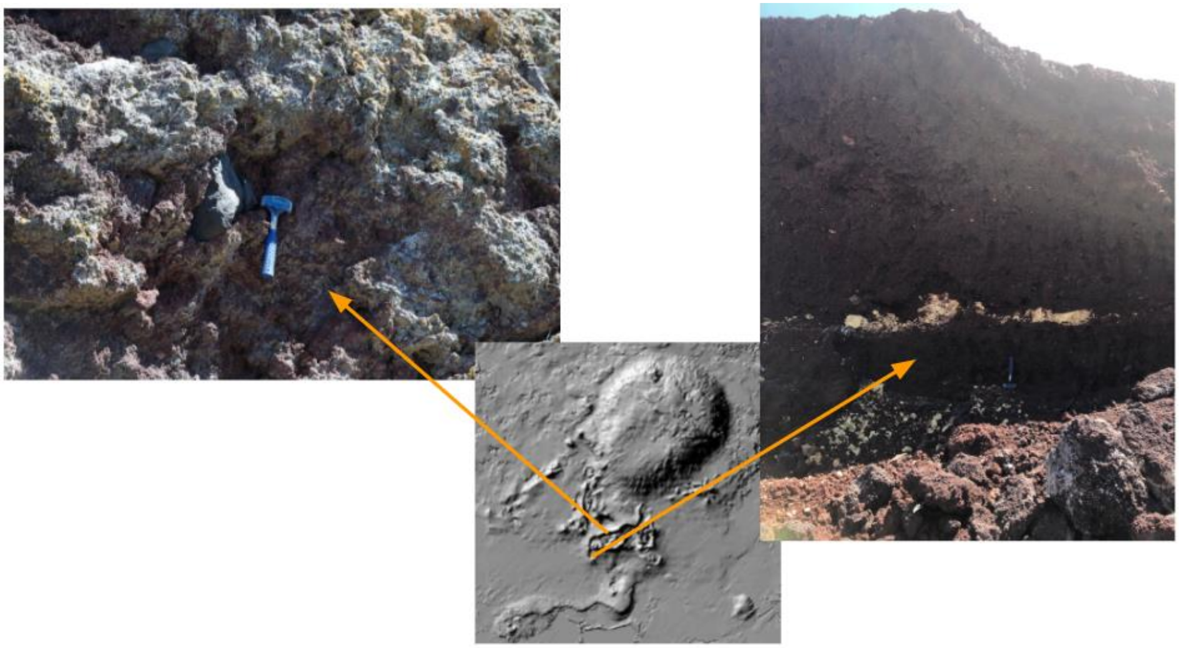

Figure 3.6: Field photos taken from the east to west trend of the breaks showing the lithology inside the outcrops with the different clasts and phreatomagmatic properties.

Previous maps of the area do not differentiate The Breaks from Table Butte, simply treating is as an extension of the main edifice and area of very high vent density (ex., Kuntz et al., 1994). Although past work has indicated concerns that The Breaks may be littoral cones from lava emplacing over wet ground or interacting with a shallow lake (Hughes et al., 2000), the vents in The Breaks have continued to be treated as primary vents from Table Butte (ex., Gallant et al., 2018). We interpret the layers of The Breaks to have been emplaced mostly as spatter from fissures, with occasional external water interaction causing phreatomagmatic explosions. In addition to the prevalence of spatter and near-vent spatter-fed lava facies, the interpretation of emplacement via a fissure is supported by the observed symmetry of the layers on either side of the linear trends; had The Breaks been formed by littoral blasting from a lava flow traversing wet ground, there would have likely been stiffening and subsequent inflation of the lava between its source and the explosion pits. As such, we interpret the vents of The Breaks to be primary rather than rootless. According to the procedures set forth for this project to align with the Hackett et al.

(in prep) vent dataset, we used the circular crater shapes in the interior cliffs of The Breaks to map a series of overlapping vents rather than describing each entire fissure as a single vent (Fig. 3.7). There are seven such vents for the east-west trend; the more eroded, and presumably older, north-south trending area lacked the same crater preservation and was mapped as two vents. The north-south trending portion of The Breaks is locally overlain by the main Table Butte edifice in the north and the east-west trending Breaks in the south.

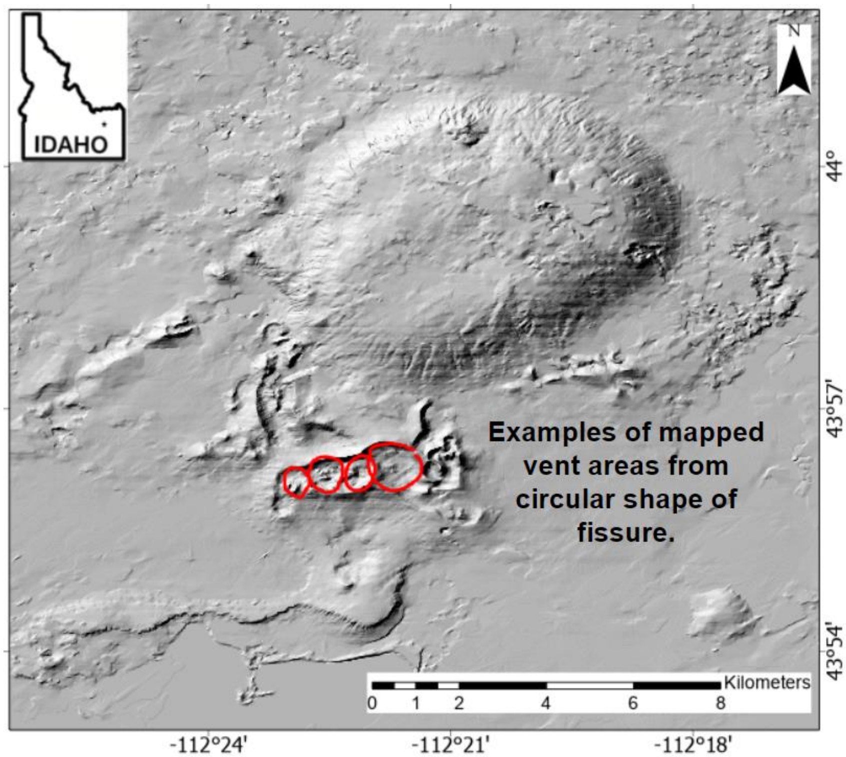

Figure 3.7: Examples of the areas that make up the circular morphology and describe the point at which a vent was created for the vent dataset.

The Needle Butte trend sits to the west of Table Butte with a northeast-southwest lineation of five vents. These vents are visible in aerial imagery as positive topographic features along with the trend; spatter was observed at the vents in the field. We interpret this area as having been emplaced during a single fissure eruption that concentrated into five-point sources now identifiable as vents. The Needle Butte trend underlies the main Table Butte edifice.

The final morphologic area is the main edifice of Table Butte. The main edifice has three vents that form a northwest-southeast line after mapping was completed with updated vents; this represents an increase from the two vents previously included in Kuntz et al. (1994). The vent areas did not display any phreatomagmatism, nor did any other section of the main edifice. All three vents had accumulations of spatter and spatter-fed lava, and the middle and southern vents also had well-developed lava channels draining to the southeast; the channel from the southern vent drained out into a broad flow on the flat land adjacent to the steep-sided main edifice. The lava layers on the main edifice were generally only a meter or less thick, with shelly pahoehoe morphologies exposed in the near-vent channels. There was a ~1 m tall step in topography that ran approximately north-south across the top of the main edifice where one of the later lava flows ceased flowing westward; the lavas on either side of that step had different phenocryst content, discussed in subsequent sections. Other small topographic steps on the main edifice may also be related to flow unit terminations but were harder to identify in the hillshade due to small sand dunes. Deep gullies in the northwestern margin of the main edifice exposed a thick (>20 m) stack of thin lava flow units with increased red oxidation, rounded weathering, and noticeably higher phenocryst content than in the overlying lavas.

3.4.2 Lava descriptions

The lavas of the Table Butte area were divided into four categories based on mineral modes and were informally named Quaternary Table Butte Basalt 1-4 during field work (Table 3.2). Rock unit Qtbb1, located in the Needle Butte trend and the north-south oriented portion of The Breaks, is ~7% plagioclase phenocrysts up to 2 mm in length and has trace olivine up to 1 mm. Qtbb2, the next unit stratigraphically, contains more than 20% olivine glomerocrysts 5-10 mm across, with 2% 1-2 mm plagioclase phenocrysts. This unit, only observed in the deeply incised gullies on the northern margin of the main Table Butte edifice, was noteworthy for its pervasive red oxidation color that increased with depth and the weathering pattern of the unit into rounded surfaces. Qtbb3 directly overlies Qtbb2 on top of Table Butte and makes up the east-west trending portion of The Breaks. It has trace amounts of both plagioclase and olivine phenocrysts, mostly under 1 mm in size. The final unit, Qtbb4, is the uppermost unit on the eastern half of Table Butte and extends down onto the flats to the east. It contains 4-5% olivine phenocrysts (up to 2 mm across) and trace plagioclase (Table 3.2, Fig., 3.8).

Table 3.2: Field descriptions of the rock units and associated sample numbers. Note that not all samples were used in petrographic and XRF analyses.

Unit Name	Samples	Description
Qtbb1	CB-1, NB-3, BR-2, BR-3, BR-4, BR-5	Quaternary Table Butte Basalt 1 (Pleistocene?) - Contains plagioclase approximately 5% of rock and 2-3 mm in size, and olivine crystals taking up less than 2% of the rock around 2mm in size. (No age data).
Qtbb2	TB-3, TB-11, TB-13, TB-14, TB- 15, TB-16, TB-17, TB-18, TB-19, TB-21-SKN1, TB-21-SKN2, TB-21-SKN3	Quaternary Table Butte Basalt 2 (Pleistocene?) - Contains olivine glomerocrysts up to 10% of rock and up to 10mm in length. Plagioclase was less than 1% of rock up to 2mm in length. (No age data).
Qtbb3	TB-6, TB-9a, TB-9b, TB-22, TB-23, TB-25, TB-27, TB-28	Quaternary Table Butte Basalt 3 (Pleistocene?) - Contains plagioclase 2% of rock and up to 3 mm in size, and olivine at 2% of rock and 2mm in size as singular crystals. (No age date for this unit).
Qtbb4	BR-1, NB-1, NB-2, TB-1, TB-2, TB-4, TB-5, TB-8, TB-10, TB-20, TB-21, TB-26	Quaternary Table Butte Basalt 4 (Pleistocene)- Contains plagioclase less than 1% of rock around 1-2mm in size and olivine less than 1% of rock 1-2 mm in size as singular crystals. (Ar Age date 392 ka by B. Turrin)

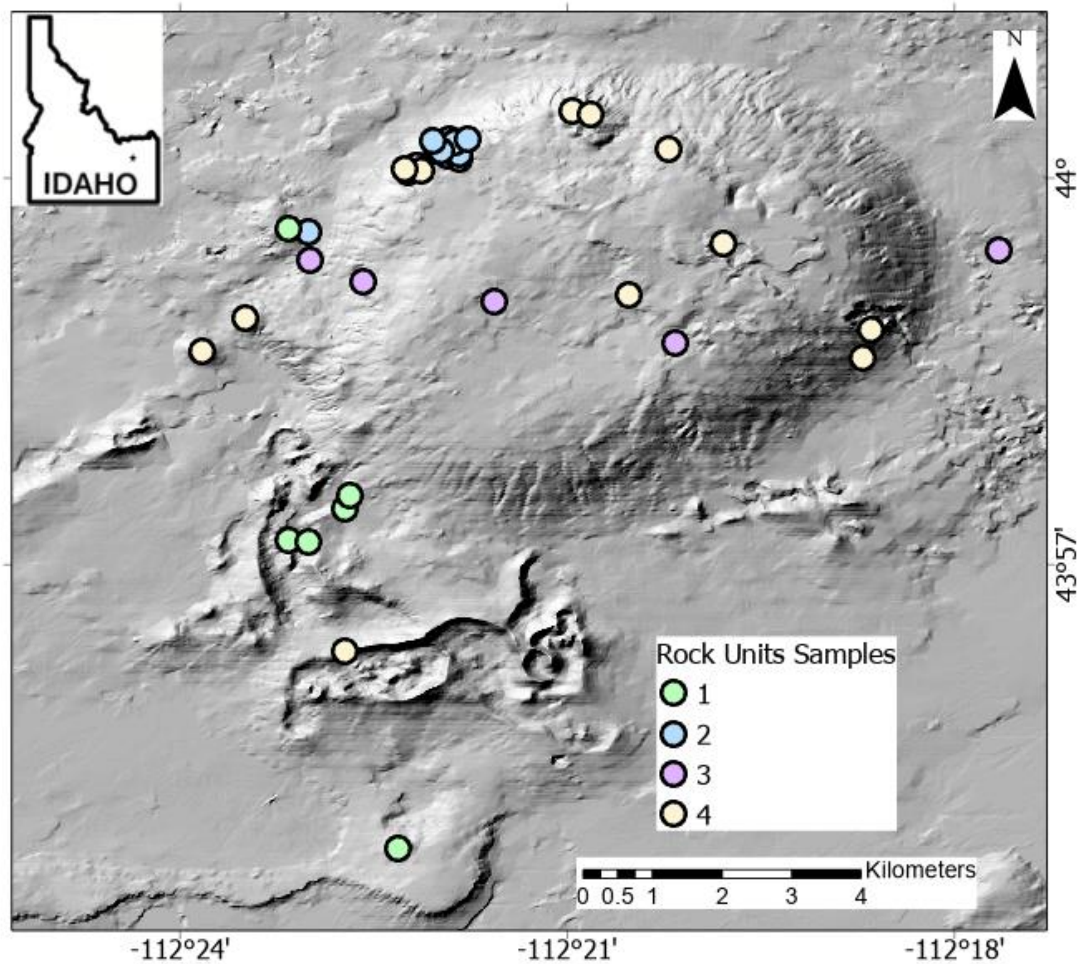

Figure 3.8: Map of field classification of samples. See Table 3.2 for field descriptions.

Complete point counts of the samples aligned with the field descriptions of the units (Table 3.3). Although 1000 points were counted on each slide, 12-51% (mean 24%) of the points for any individual slide were void space/secondary infill and were thus removed from the normalized count. As a result, the functional number of points counted per slide ranged from 493 to 883 (mean 756). Thus, the error in the calculated mineral percentages is approximately +/- 1.5-2.5% (or up to ~50% relative error), depending on the true mineral percentage and the points counted for a specific thin section (Van der Plas and Tobi, 1965). As such, two of the samples could not confidently be classified in any of the four lava types based on petrographic analysis alone.

Table 3.3: Percentages of plagioclase, olivine, and matrix, sorted into different rock units depending on the percentages. While all thin section analyses were originally conducted with 1000 points per slide, void space and secondary infill were subsequently removed, and the points were renormalized. Error values were determined using the nomogram of Van Der Plas and Tobi (1965). The colors classify the different rock units across the multiple tables and maps following this point, red= Qtbb1, orange= Qtbb2, green= Qtbb3, blue= Qtbb4, gray= unknown groups.

Rock Unit	Sample	Plagioclase %	Olivine %	Matrix %	Points counted
Qtbb1	BR-2	6.8 +/- 1.6	2.3 +/- 0.9	90.9 +/- 2.1	818
	BR-3	6.0 +/- 1.5	0.2 +/- 0.1	93.8 +/- 2.0	738
	NB-1	10.3 +/- 2.4	2.3 +/- 1.2	87.4 +/- 2.6	614
	NB-2	8.3 +/- 2.5	1.5 +/- 0.5	90.2 +/- 2.7	493
	NB-3	6.6 +/- 1.6	1.9 +/- 0.6	91.5 +/- 2.2	736
Qtbb2	TB-3	2.3 +/- 0.4	22.6 +/- 2.9	75.1 +/- 3.2	784
Qtbb3	BR-1	0.2 +/- 0	1.0 +/- 0.1	98.8 +/- 0.5	685
	TB-23	0.1 +/- 0	0.4 +/- 0	99.5 +/- 0.1	779
Qtbb4	TB-2	0	3.3 +/- 0.8	96.7 +/- 1.2	903
	TB-5	0	6.3 +/- 1.8	93.7 +/- 2.0	646
	TB-10	0.4 +/- 0.1	2.3 +/- 1.0	97.4 +/- 0.7	800
	TB-14	0.7 +/- 0.1	5.4 +/- 1.3	93.9 +/- 0.9	883
	TB-17	0.1 +/- 0	4.2 +/- 1.0	95.7 +/- 1.4	792
	TB-20	0	2.5 +/- 1.0	97.5 +/- 1.1	764
	TB-21	0	3.9 +/- 1.1	96.1 +/- 1.3	698
	TB-26	0.7 +/- 0.1	5.8 +/- 1.2	93.5 +/- 1.7	843
Unknown	CB-1	2.0 +/- 1.9	1.4 +/- 0.7	96.6 +/- 1.3	876
	TB-25	2.1 +/- 0.9	3.9 +/- 1.0	94.1 +/- 1.9	713

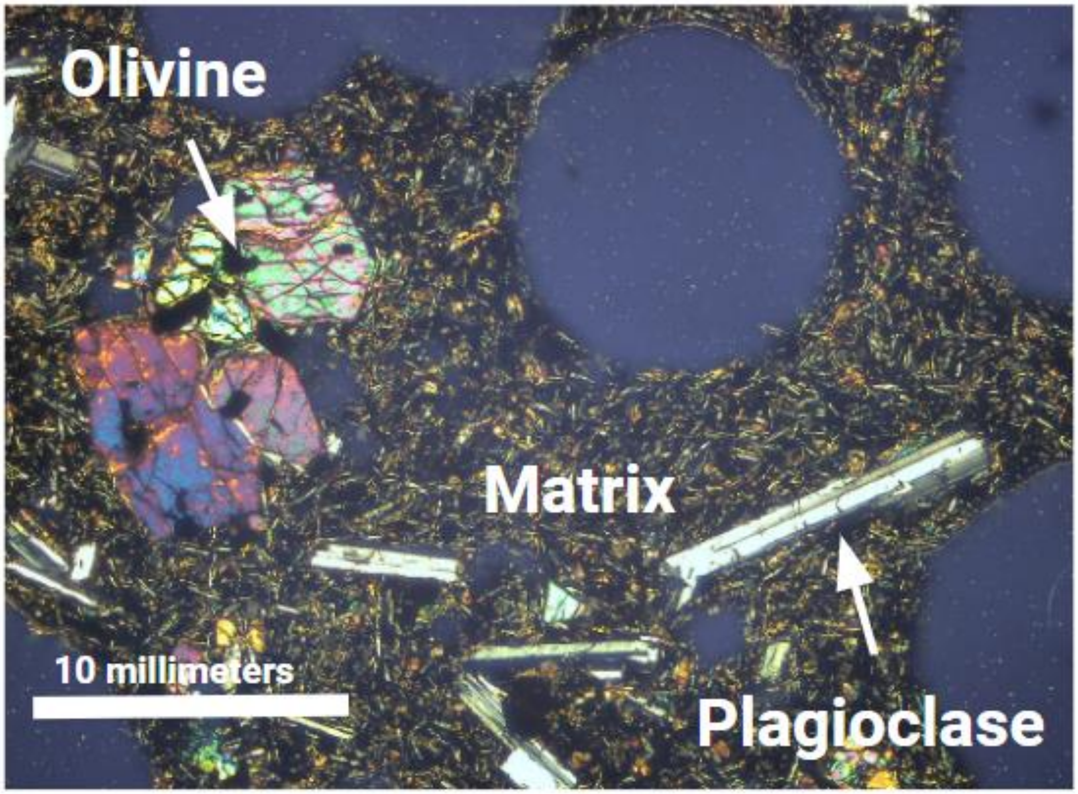

Figure 3.9: Sample image of mineral modes considered during the point counting. This image is from sample NB-1. The slide photo was taken under magnification of 20x and cross-polarized light.

Table 3.4: Major element oxides of samples as measured by XRF.

Sample	SiO2	TiO2	Al2O3	Fe2O3	FeO	MnO	MgO	CaO	Na2O	K2O	P2O5	Total
	mass %	mass %	mass %	mass %	mass %	mass %	mass %	mass %	mass %	mass %	mass %	mass %
BR-1	45.1	2.95	14.9	16.7	15.0	0.220	7.26	10.6	2.82	0.730	0.350	100
BR-2	47.6	3.39	14.3	16.3	14.6	0.229	6.04	9.47	2.65	1.07	0.610	100
BR-3	47.3	3.82	14.5	17.4	15.7	0.232	5.58	8.72	2.75	1.06	0.420	100
CB-1	46.1	3.44	14.2	16.8	15.2	0.234	6.30	9.81	3.05	1.13	0.550	100
NB-1	46.5	3.95	14.0	17.3	15.6	0.233	5.78	9.39	2.73	1.05	0.760	100
NB-2	46.9	3.89	14.1	16.9	15.3	0.233	5.66	9.47	2.81	1.04	0.710	100
NB-3	45.8	3.98	13.4	17.9	16.2	0.246	5.95	9.86	2.76	1.04	0.760	100
TB-2	46.7	2.46	14.6	14.8	13.3	0.214	8.95	10.5	2.33	0.520	0.440	100
TB-3	46.5	1.87	15.5	14.4	12.9	0.193	9.08	11.3	2.13	0.320	0.210	100
TB-5	47.3	2.38	15.0	14.3	12.9	0.193	8.89	10.3	2.20	0.549	0.301	100

TB-10	46.9	1.77	16.0	13.5	12.2	0.183	8.81	11.3	2.20	0.315	0.209	100
TB-14	46.6	1.90	15.8	14.1	12.7	0.193	8.39	11.7	2.20	0.305	0.201	100
TB-17	46.1	1.90	15.3	14.8	13.3	0.203	9.19	11.5	2.13	0.284	0.198	100
TB-20	46.6	2.19	15.1	14.1	12.7	0.204	9.29	10.9	2.24	0.428	0.417	100
TB-21	47.2	2.49	14.6	14.5	13.0	0.214	8.74	10.3	2.34	0.633	0.471	100
TB-23	46.8	2.74	14.9	15.8	14.2	0.214	6.81	11.1	2.36	0.499	0.372	100
TB-25	45.8	2.59	15.1	16.0	14.4	0.214	8.15	10.8	2.28	0.376	0.282	100
TB-26	46.4	2.20	15.3	14.0	12.6	0.202	9.43	10.8	2.35	0.374	0.352	100

Table 3.5 Minor element concentrations of the samples as measured by XRF.

Sample	Ba	Ce	Cl	Cr	Cu	F	Ga	La	Nb	Nd	Ni	Pb	Rb	S	Sc	Sm	Sr	Th	U	V	Y	Zn	Zr
	ppm	ppm	ppm	ppm	ppm	ppm	ppm	ppm	ppm	ppm	ppm	ppm	ppm	ppm	ppm	ppm	ppm	ppm	ppm	ppm	ppm	ppm	ppm
BR-1	353	31	286	167	37	383	17	8	18	27	69	4	10	100	25	6	264	2	0	240	23	105	194
BR-2	673	59	452	97	35	668	19	19	30	43	71	8	23	214	24	8	300	4	1	247	32	137	321
BR-3	591	55	2418	66	33	650	21	14	34	44	48	7	23	24	27	9	288	3	0	253	28	155	350
CB-1	489	54	676	104	34	355	18	17	30	41	93	8	21	339	25	8	291	3	0	244	31	136	313
NB-1	591	79	242	78	30	479	20	24	35	58	47	7	18	41	28	10	315	2	0	312	42	146	375
NB-2	550	68	375	73	34	676	21	17	34	47	47	7	19	922	27	7	295	4	1	295	38	141	363
NB-3	549	69	890	65	33	664	20	19	34	51	40	7	16	457	25	9	289	3	0	286	39	144	354
TB-2	314	36	749	304	40	431	18	13	20	32	103	5	9	229	28	6	233	2	0	261	26	106	231
TB-3	227	24	217	310	47	226	18	11	11	25	117	3	5	108	29	4	215	1	0	239	19	104	141
TB-5	345	31	294	318	40	397	18	10	16	31	116	5	13	82	29	7	253	2	0	255	26	111	173
TB-10	244	28	232	274	45	224	18	12	11	20	104	4	5	241	26	4	218	0	0	214	19	100	134
TB-14	243	25	145	255	50	236	18	9	11	19	89	2	6	52	29	5	216	0	0	236	19	96	136
TB-17	297	18	238	293	43	418	18	11	11	21	100	5	5	483	28	4	215	2	0	225	18	100	139
TB-20	377	38	264	363	35	433	18	15	18	30	123	6	7	131	30	4	242	3	0	270	25	103	213
TB-21	441	46	350	259	36	545	18	18	22	34	107	6	13	656	27	6	258	2	0	259	28	115	253
TB-23	432	47	145	211	45	484	20	16	19	40	56	7	9	1057	30	6	275	3	0	286	29	130	224
TB-25	355	36	328	230	38	475	20	10	18	30	74	4	5	1025	28	6	270	1	0	261	23	123	205
TB-26	272	36	311	414	43	361	18	12	18	32	137	4	6	87	31	6	246	2	0	282	24	108	218

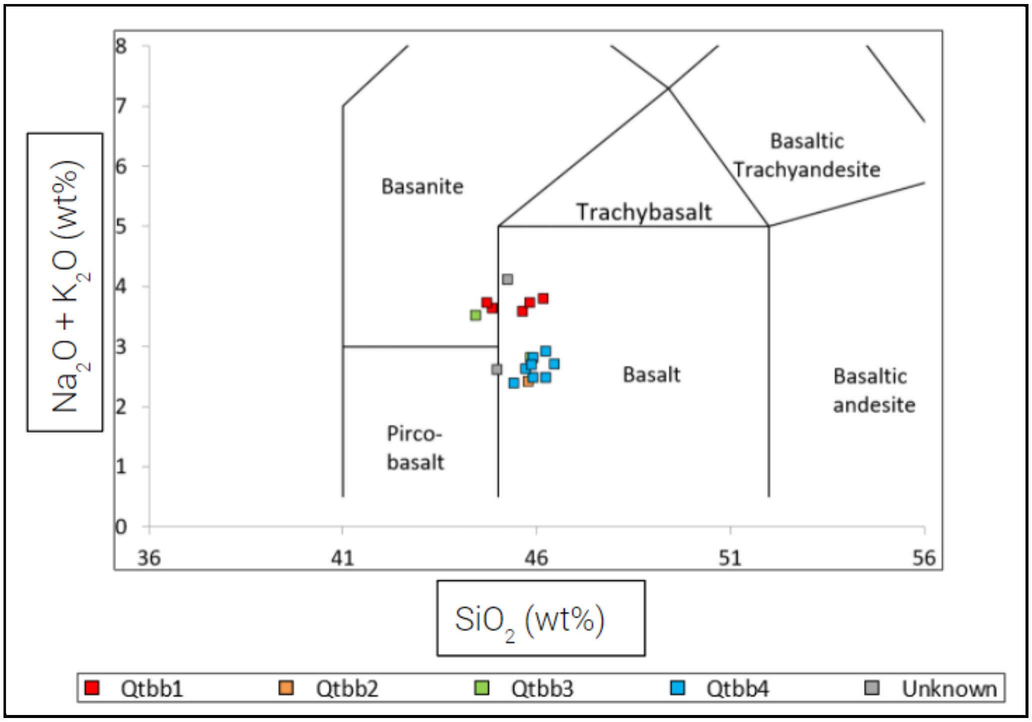

Figure 3.10: TAS diagram of the 18 rock samples color-coded based on identification from petrographic analyses (note that the two samples that could not be confidently classified are listed as "unknown"). The alkali-rich cluster of points represents those samples with increased plagioclase content.

XRF geochemical data is listed in Tables 3.4 and 3.5. Fenner diagrams of major element oxides and minor elements (Fig. 3.11) illustrate Qtbb1 and Qtbb2/4 as end members of distribution, with Qtbb3 serving as the transitional unit. The samples designated as unclassified based on petrographic point count analyses sit near the ends of the intermediate transitional zone. Conducting multivariate analysis of the plagioclase and olivine counts and the major and minor elements reinforces the division of the sample suite into four types (Fig. 3.12) and indicates that the unclassified sample CB-1 best fits with Qtbb1, while TB-25 belongs with Qtbb3 (Table 3.6). These classifications make sense spatially, with CB-1 aligned with the Qtbb1 in the north-south trending area of The Breaks and TB-25 coming from the southwest portion of the main edifice, the same as the rest of unit Qtbb3 (Fig. 3.13).

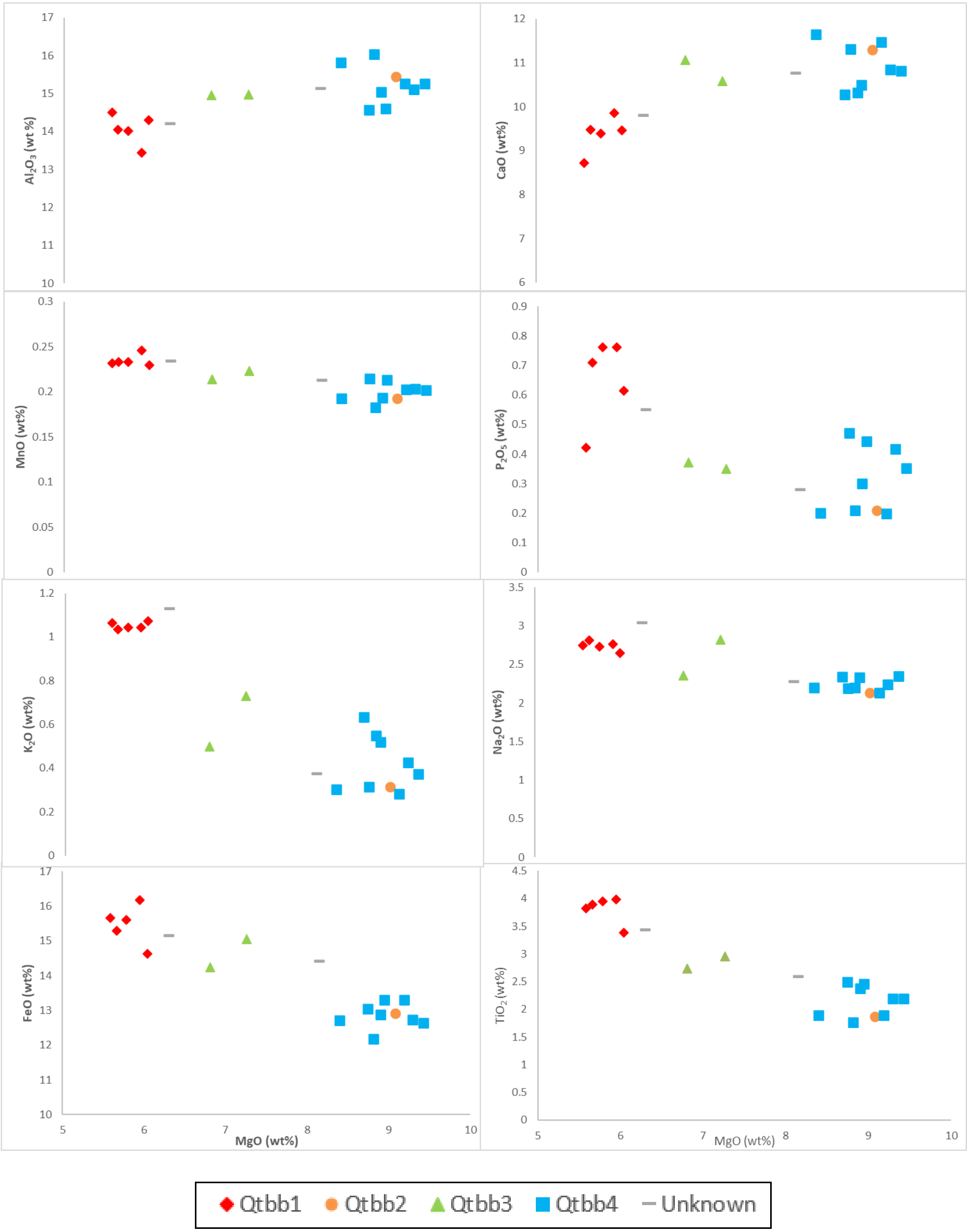

Al_2O_3 (wt %)
CaO (wt%)
MnO (wt%)
P_2O_5 (wt%)
K_2O (wt%)
Na_2O (wt%)
FeO (wt%)
TiO_2 (wt%)
MgO (wt%)
Qtbb1
Qtbb2
Qtbb3
Qtbb4
Unknown

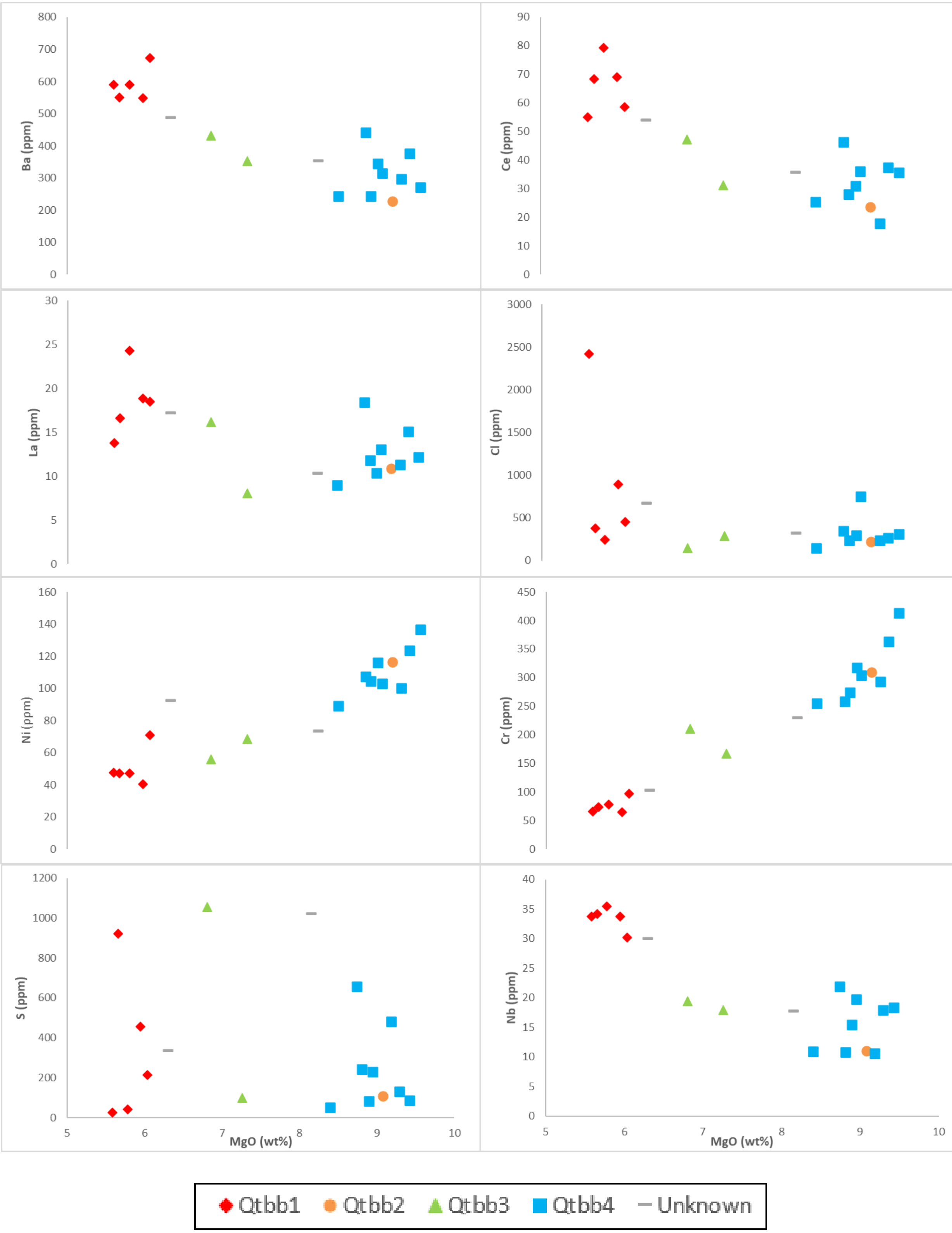
Ba (ppm)
Ce (ppm)
La (ppm)
Cl (ppm)
Ni (ppm)
Cr (ppm)
S (ppm)
Nb (ppm)
MgO (wt%)
MgO (wt%)
Qtbb1
Qtbb2
Qtbb3
Qtbb4
Unknown

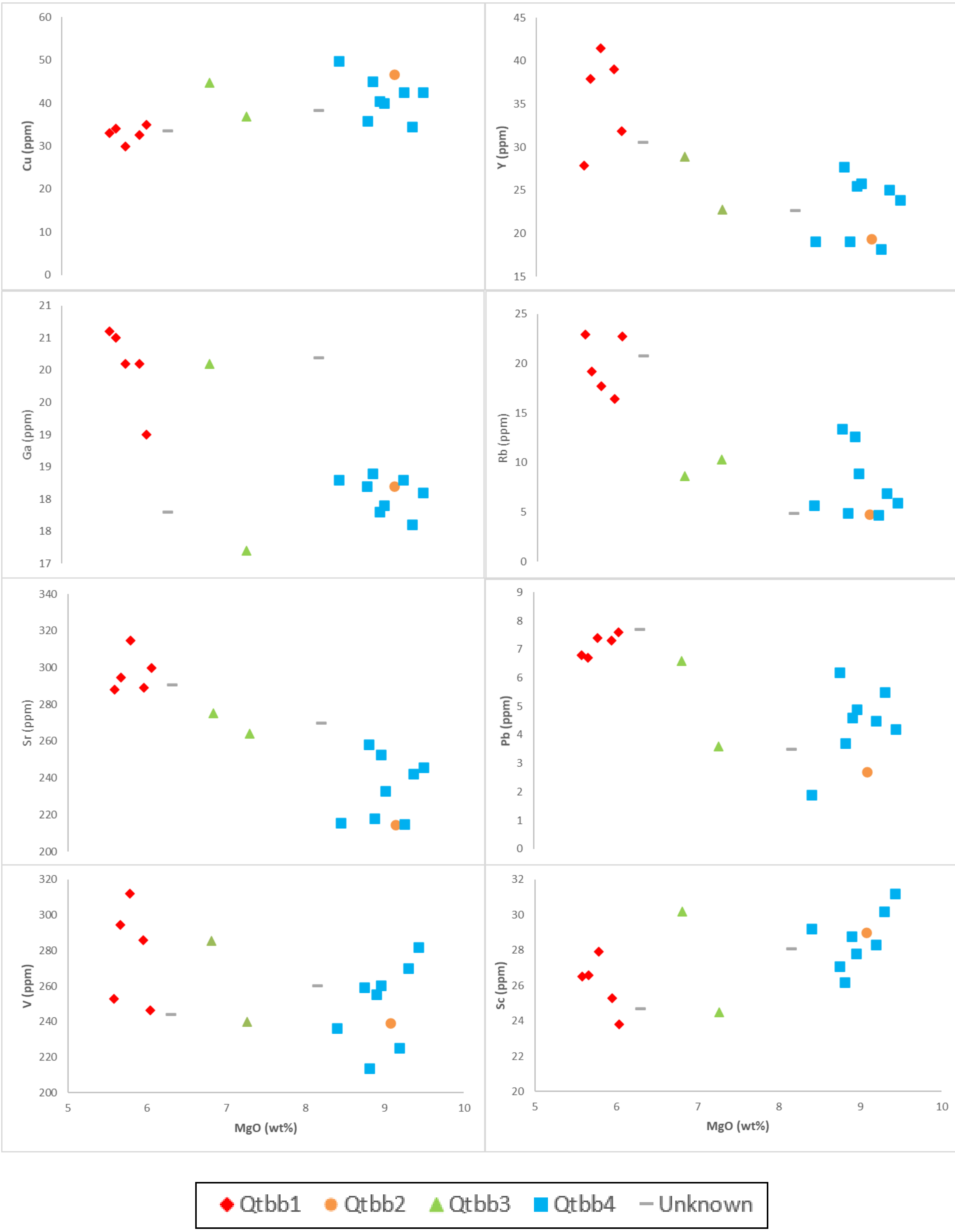
Cu (ppm)
Y (ppm)
Ga (ppm)
Rb (ppm)
Sr (ppm)
Pb (ppm)
V (ppm)
Sc (ppm)
MgO (wt%)
MgO (wt%)
Qtbb1
Qtbb2
Qtbb3
Qtbb4
Unknown

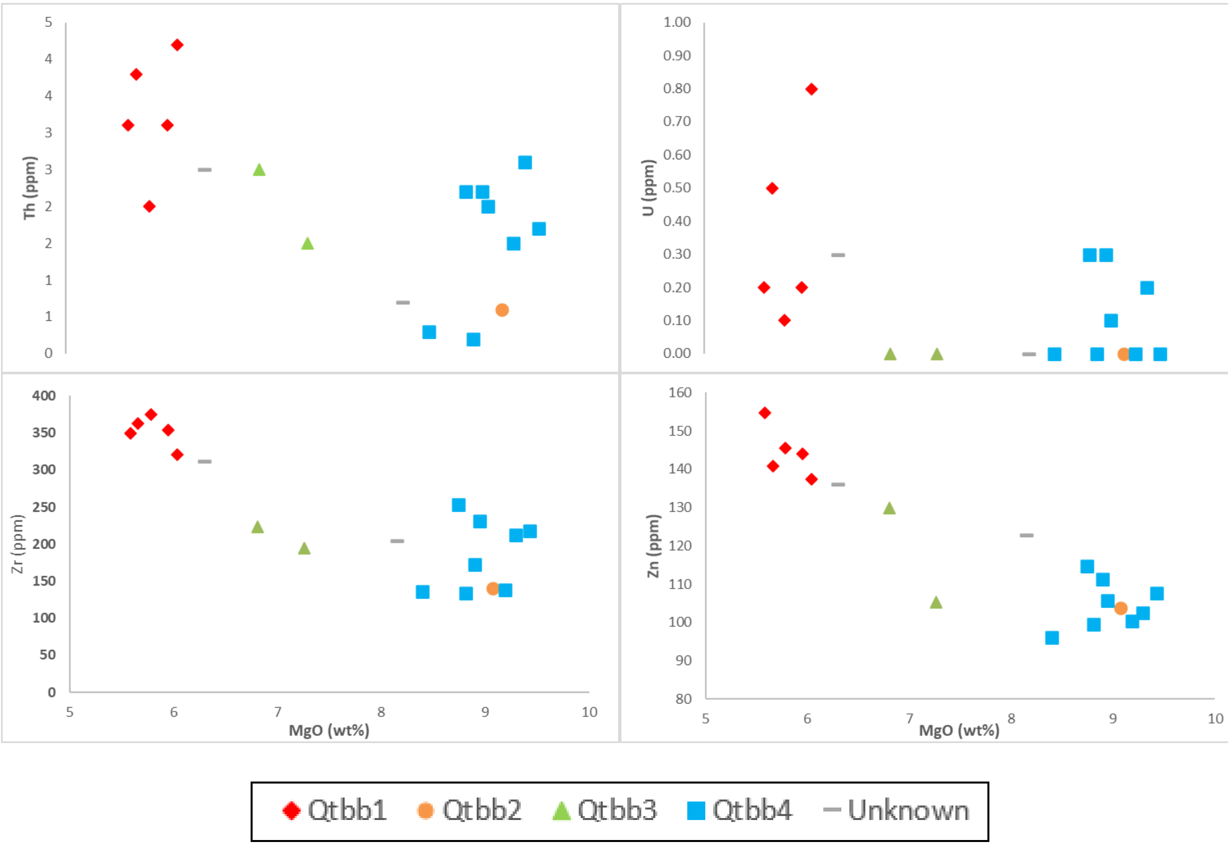

Figure 3.11: Fenner diagrams displaying the rock samples and into groups with the unknowns still showing transitional units along with Qtbb3. Note the graphs shown best represent the data set all other diagrams contained in the appendix.

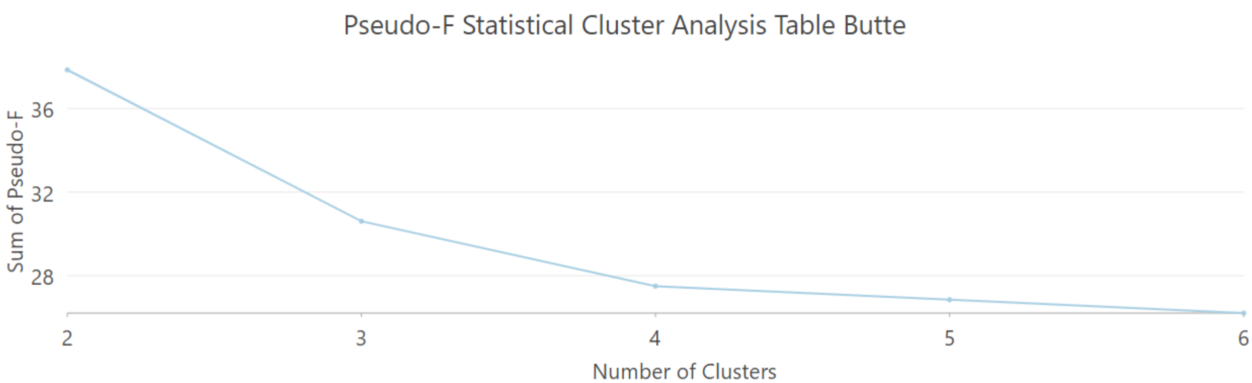

Figure 3.12: Elbow chart from the Pseudo-F statistical cluster analysis of the different geochemistry and point count analysis. The break in slope at four on the x-axis indicates the appropriate number of clusters to use when categorizing the dataset.

Table 3.6: Samples broken down into separate multivariate clusters. The divisions reinforce the tentative field identification of four units and allow classification of samples that had been considered marginal between groups.

Qtbb1	Qtbb2	Qtbb3	Qtbb4
BR-2-SW	TB-3-SW	BR-1-SW	TB-2-SW
BR-3-SW		TB-23-SW	TB-5-SW
CB-1-SW		TB-25-SW	TB-10-SW
NB-1-SW			TB-14-SW
NB-2-SW			TB-17-SW
NB-3-SW			TB-20-SW
			TB-21-SW
			TB-26-SW

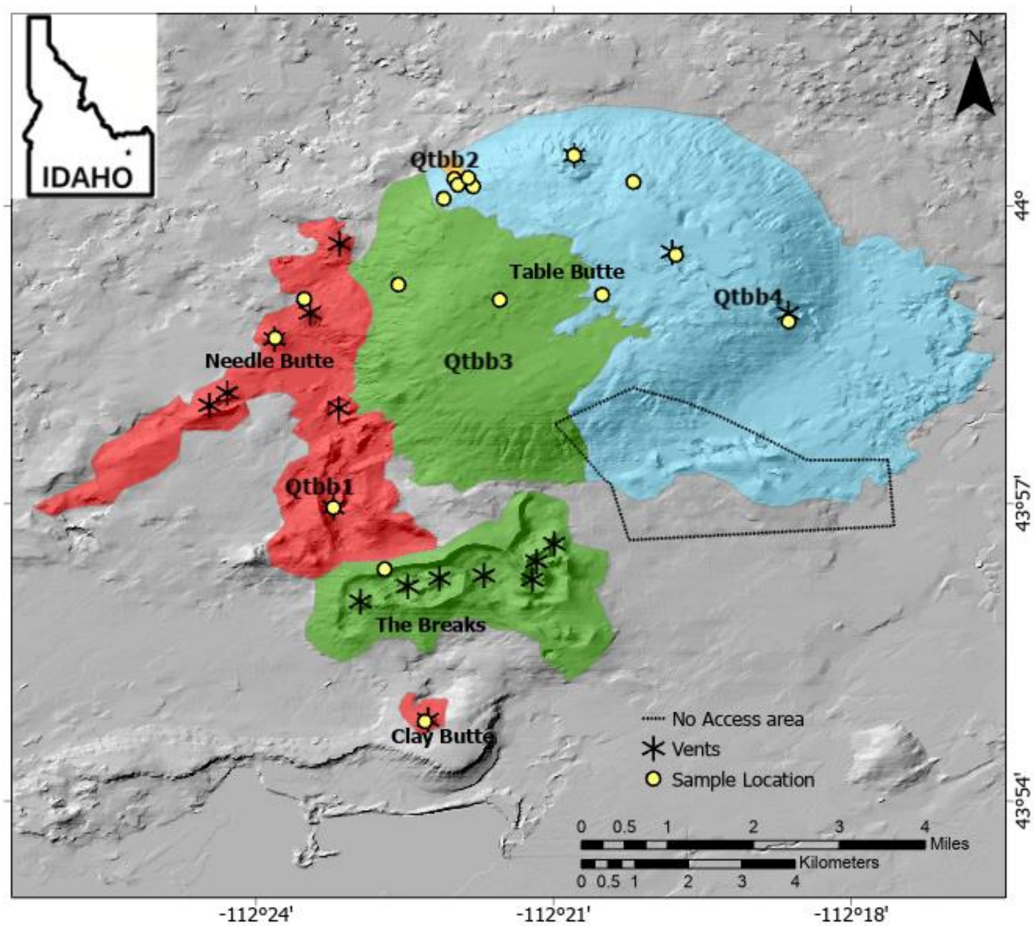

Figure 3.13: Map of the multivariate-clustered samples classifications into four rock units. The multivariate analysis used the olivine and plagioclase mineral percentages from point counting and the major element oxide and minor element values from XRF.

3.5 Discussion

3.5.1 Geologic history of Table Butte

The Table Butte eruptive sequence started with the emplacement of Qtbb1 through two subparallel fissures: the Needle Butte trend and the north-south oriented portion of The Breaks. The latter area interacted with limited external water, either as shallow surface water or groundwater, triggering phreatomagmatic pulses within the dominantly spatter-driven eruption. Based on the surface topography of the north-south portion of The Breaks and the distinct lithology of Qtbb1, we interpret this to have been a separate eruptive event from the subsequent emplacement of the other lavas.

Qtbb2, Qtbb3, and Qtbb4 were erupted in sequence and came from the main edifice of Table Butte; Qtbb3 also erupted from the fissure that formed the east-west oriented portion of The Breaks. As during the Qtbb1 eruptive event, the Qtbb3 fissure in The Breaks was mostly spatter and spatter-fed lava, with occasional exposure to external water to trigger phreatomagmatic blasts. We did not observe any evidence of phreatomagmatism such as palagonite or tuff on the main edifice itself, with almost the entire edifice draped by thin (down to sub-meter thick) lava flows of Qtbb3 and Qtbb4. While Qtbb2 displayed more weathering than the overlying units, there was no compelling evidence that this was the result of increased water-lava interaction. Neither was there any other clear indication of external influences that would explain the unusual steep sides and flat top of the main Table Butte edifice. We are left with two plausible hypotheses: 1) burial of a phreatomagmatically-affected, steep-sided unit by subsequent dry lava and 2) uplift by cryptodome instead of constructional lava emplacement. Testing of these hypotheses will require further research through geophysical surveys or drill core.

The main edifice of Table Butte is similar in shape and scale to Buckskin Butte, a cryptodome located on the southeastern margin of the ESRP on the Fort Hall Reservation. However, Buckskin Butte, Ferry Butte, and Middle Butte, all recognized cryptodomes on the ESRP, are characterized by disruption of the original basalt surface. This disruption is visible in topographic data and aerial imagery as deep cracks and tilted lava platforms, with profound erosion gullies on the steep flanks due to the vulnerability triggered by the cracking. Although none of these characteristics are observable at Table Butte, it is possible that this is a function of intrusion depth and age. More compelling as an argument against the cryptodome uplift of Table Butte, however, is the geometry of vents and their associated flow patterns: the Table Butte lavas appear to be in their original eruption geometry. As such, we prefer the hypothesis that the overall morphology of the main Table Butte edifice is due to a buried steep-sided phreatomagmatic unit that was subsequently filled and overtopped by lavas erupting in a dry environment (Figure 3.14). Future research via core hole or geophysical surveys should be able to definitively resolve this open question.

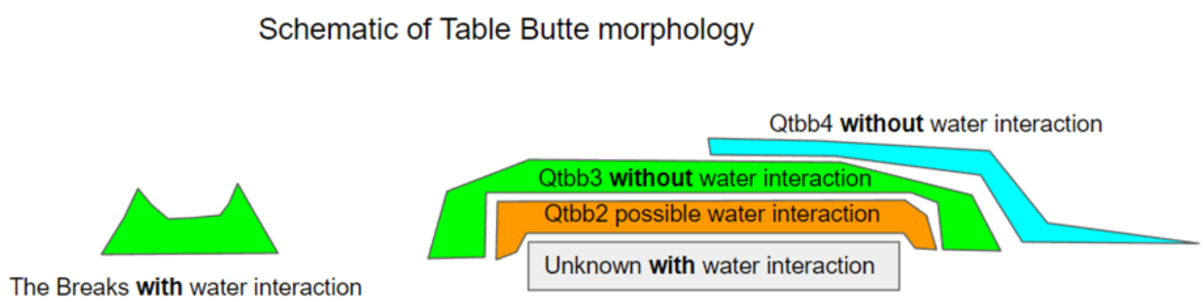

Figure 3.14: A simple schematic of the eruptive events forming Table Butte and the areas that include water interaction.

3.5.2 Vents and events

We have mapped The Breaks as a series of overlapping vents contributing to the fissure, but we recognize that this is a choice driven motivated by consistency with how the vents of the Needle Butte trend and across the top of Table Butte are mapped; another researcher might chose to represent The Breaks by a single vent per fissure, deeming the craters too far coalesced to merit differentiation. We interpret the aligned vents in The Breaks, the Needle Butte Trend, and across the top of the main Table Butte edifice as fissure eruptions. Given our choice to divide the fissures into different vents wherever viable based on crater morphology, we mapped 17 vents spanning three of the four identified lava morphologies at Table Butte; this is fewer than the 33 vents mapped by Wetmore et al. (2009) and more than the eight in Hackett et al. (*in prep*).

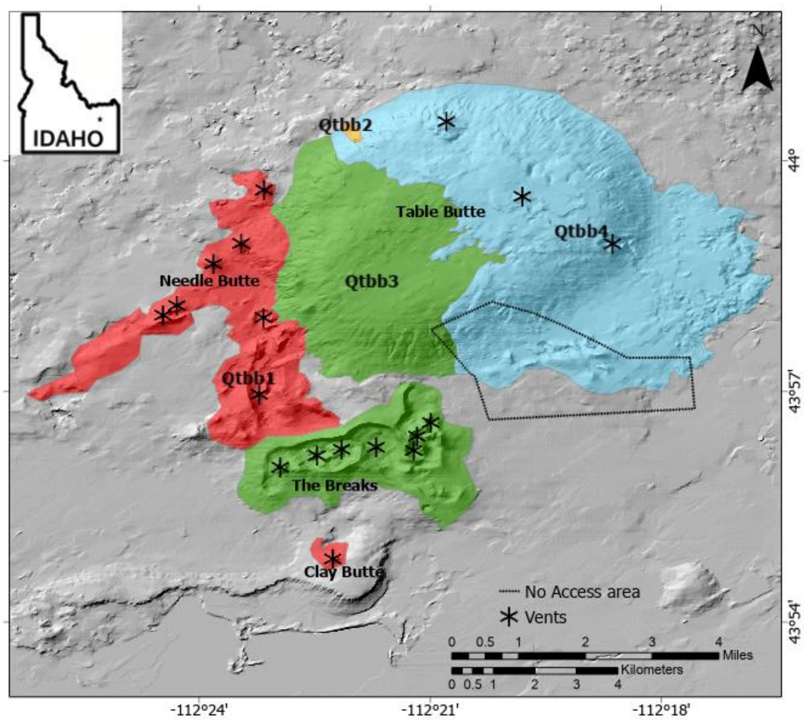

Figure 3.15: shows the rock units' location and the correlation of the vents verified with fieldwork.

Because eruptive events include all of the vents active at the same time, the Table Butte map reduces to only two event locations: the first corresponding to the emplacement of Qtbb1

(Needle Butte trend and the north-south portion of The Breaks, extending to Clay Butte) and the second related to the eruption of Qttb2, Qtbb3, and Qtbb4 on the main edifice and the east-west portion of The Breaks (Figure 3.16). When placing event locations on a map, there is no consistent methodology for selecting the position. Although the geographic center of the associated vents or deposit extent might be appealing at the event location of choice, this creates a problem of placing an event in a location where there is no vent. In order to comply with the PVHA classification methodology, we chose to assign the event location as the southeastern-most mapped vent contributing to the event.

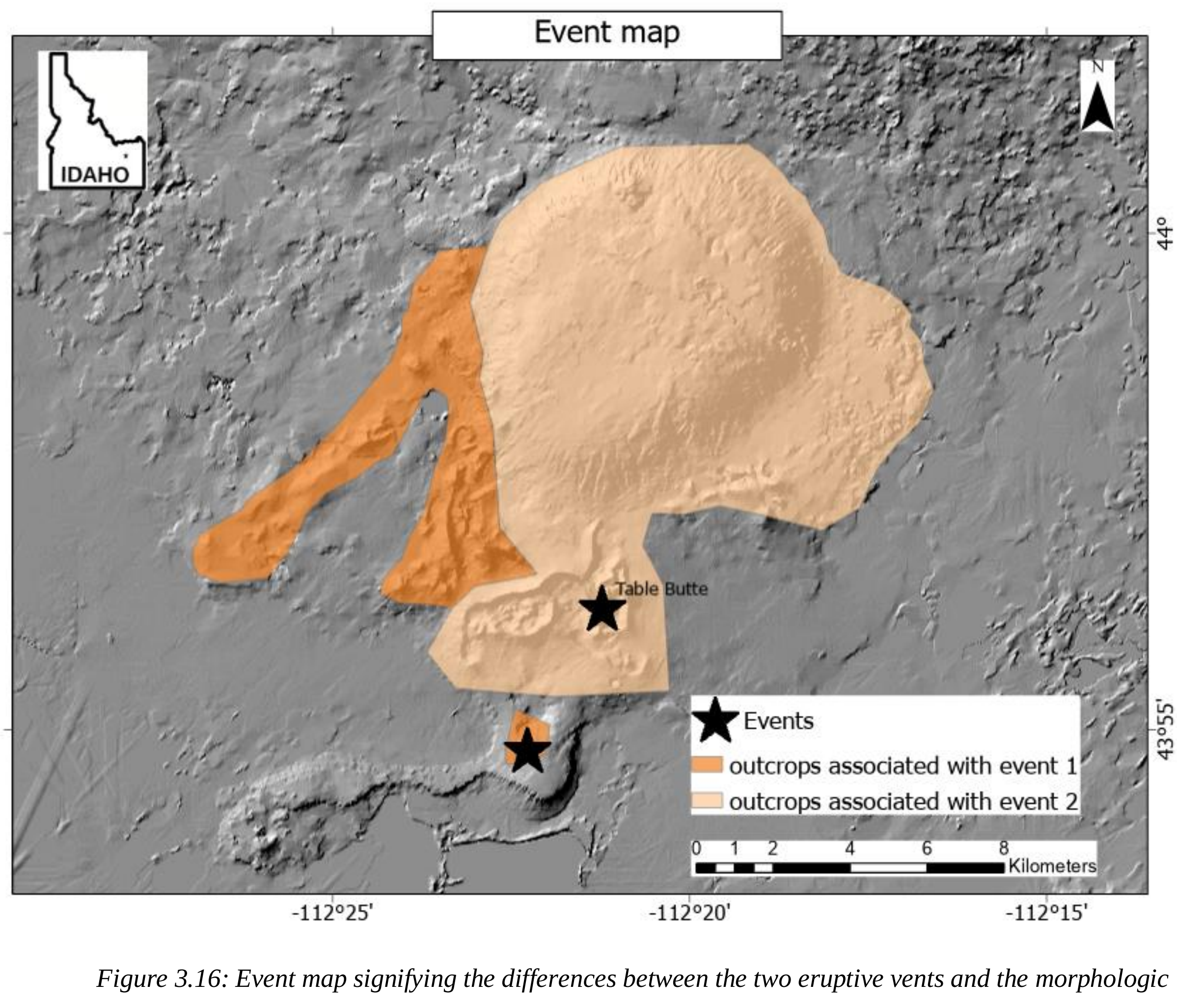

Figure 3.16: Event map signifying the differences between the two eruptive vents and the morphologic features that encompassed the two events. Transparent polygons overlay on a hillshade model created from a DEM image (USGS).

3.5.3 Hazard assessment implications

Previous work by Gallant et al. (2018) to calculate lava hazard probability for INL used MOLASSES (Modular Lava Simulation Software for Earth Sciences) with a kernel density estimation of the vent location applied to the Wetmore et al. (2009) vent data set. The 33 vents at Table Butte in that vent dataset resulted in a higher density for the Table Butte area (Gallant et al., 2018). Reducing from 33 to the 18 vents identified in this work will change the kernel density hazard analysis; this will be even further reduced by adopting an event-based spatial analysis. The kernel density estimation for predicting vent locations in a volcanic field provides the most potential area for future hazards (e.g., Connor and Connor, 2009; Connor et al., 2019). In updating the current hazards analysis, the KDE from Gallant et al. (2018) with the new and completed vent map, including the changes from Table Butte (figure 3.17).

The revised vent map and event map in development for the ESRP will provide a more accurate recurrence rate for eruptions. The recurrence rate provides two insights into a volcanic field, which involves the areas of waxing and waning through the years the volcanic field has existed and the more intense temporal trends (Condit and Connor, 1996). Updated vent and event maps for the entire ESRP are essential to improving KDE and recurrence rate models.

The Table Butte area is located in a wet subbasin with a large amount of water both in the subsurface and on the surface (Spinazola, 1994). The aquifer sits close to the surface and feeds the multiple lakes and marshland in the area, with evidence that surface water has existed over much of the last 17,000 years (Gianniny et al., 2002). Because of the clear historical record of a wet environment and the continuation of the lakes today, an eruption in the area would likely trigger at least intermitted phreatomagmatic blasting such as that observed in The Breaks at

Table Butte. This would mean a much more explosive eruptive condition that extend the area requiring rapid evacuation as part of the hazard mediation plan (Németh and Kósik, 2020).

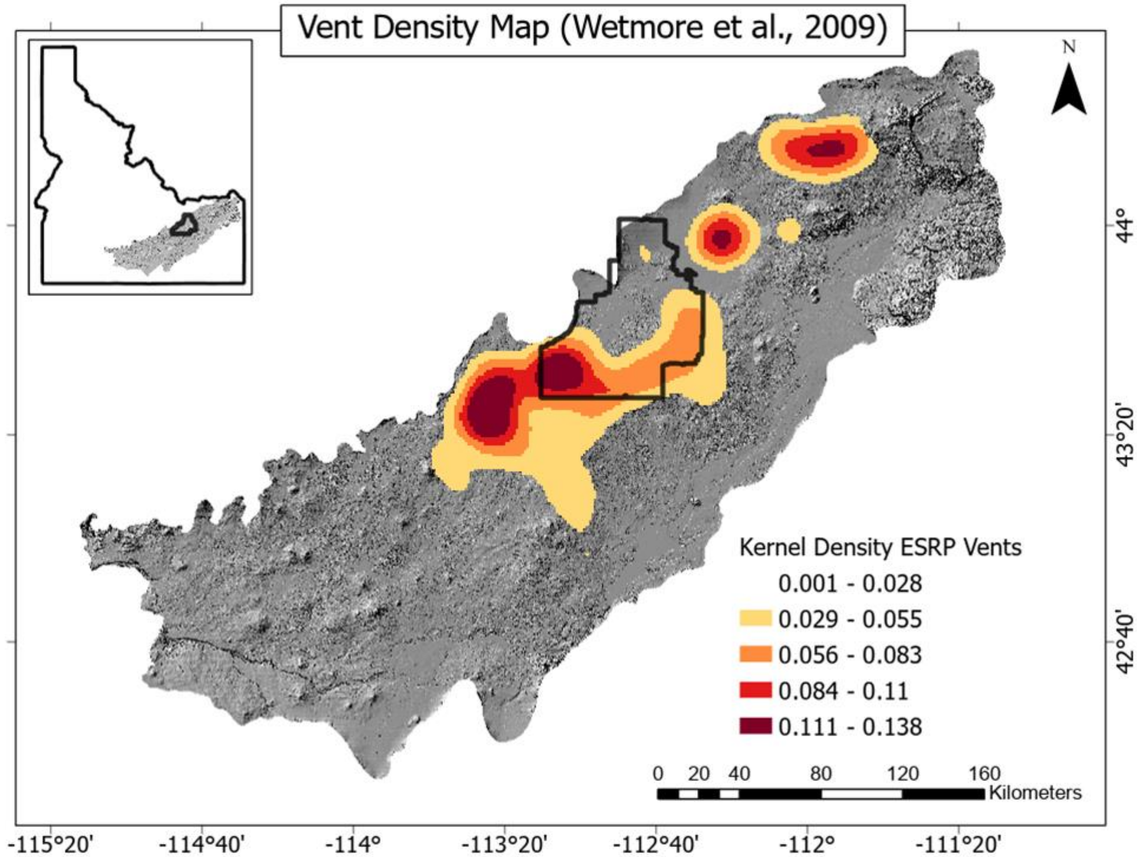

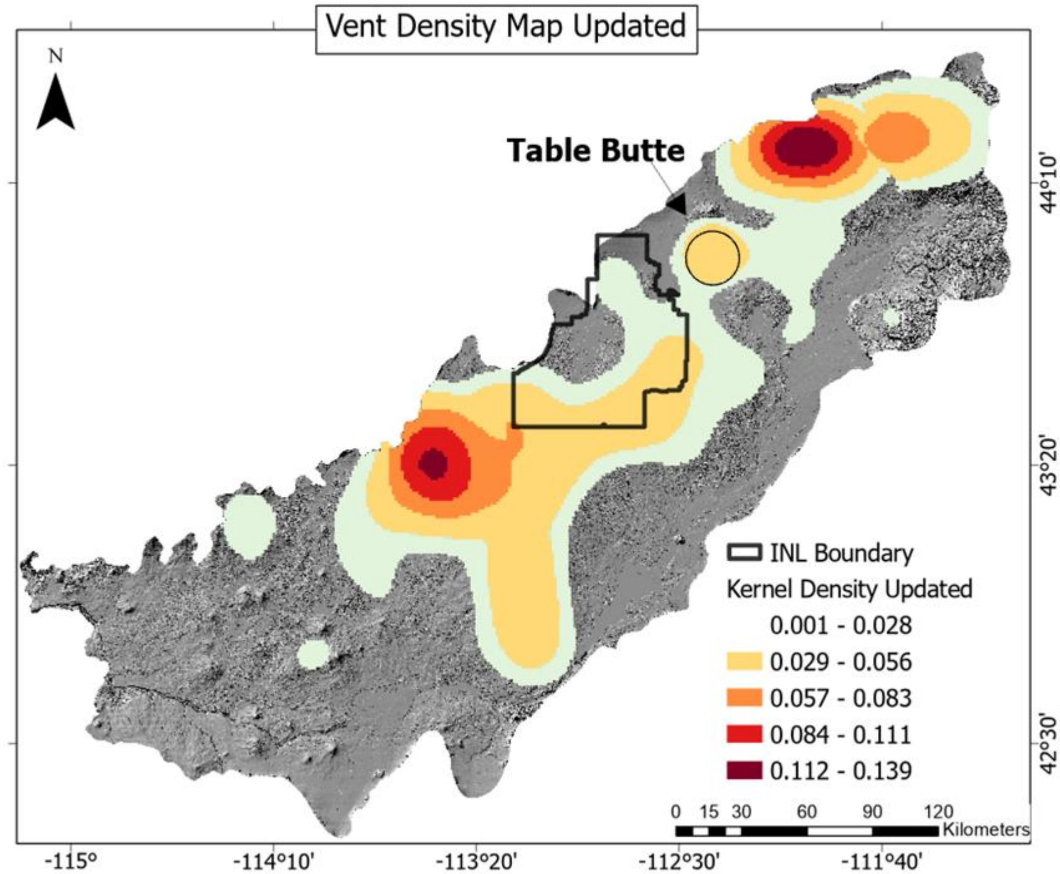

Figure 3.17: Kernel density estimation (KDE) vent maps for the ESRP. Top panel: Wetmore et al. (2009) data. Bottom panel: KDE using the Hackett et al. (in prep) dataset with the Table Butte vents updated to reflect the findings of this paper.

3.5.4 Future work

We recommend conducting geophysical surveys to study possible magnetic and gravity anomalies that could indicate whether the main Table Butte edifice morphology is a cryptodome uplifted by a basaltic or rhyolitic intrusion. Additional radiometric dating and paleomagnetic analyses could confirm whether Qtbb1 was emplaced early enough before the rest of Table Butte to merit being considered a separate event.

Future work using our revisions to the vent and event datasets will result in more accurate assessments of volcanic hazards of the Table Butte – INL area of the ESRP.

3.6 Conclusions

We conducted a detailed field study of the Table Butte volcanic system on the ESRP to answer lingering questions about the number of primary vents located there and its overall geologic history, including the role of shallow water. We collected 39 samples, 18 of which we analyzed via petrographic point counts and XRF. Based on field observations and laboratory results, there are four different lavas at Table Butte. Qtbb1 appears to predate the main Table Butte edifice and dominated by plagioclase phenocrysts. The second unit, Qtbb2, was only visible where deep erosive gullies on the northern margin of the main edifice exposed the interior of Table Butte. That unit is remarkable for its exceedingly high olivine content and more extensive weathering patterns *in situ*. Qtbb4 has the same geochemical composition as Qtbb2, though it contains a much lower crustal load. Qtbb3 has incredibly low crystallinity and represents a compositional transition between Qtbb1 and Qtbb2/4 despite being located stratigraphically between units 2 and 4. These petrologic units correspond to distinct areas in the mapped area. The last unit Qtbb4 resides only on the northeastern edge of the main edifice with a small amount of plagioclase and a slightly higher amount of olivine than in unit Qtbb3. Qtbb4 represents the last eruptive sequence as it resides as the topmost unit overlapping with Qtbb2/3.

Out of the 18 vents covering the area, Qtbb1 has eight vents organized into two different fissure orientations. Qtbb2 does not have visible vent locations due to being overlain by units Qtbb3 and Qtbb4. Unit Qtbb3 does not display any vents on the main edifice, but the east-west fissure in The Breaks contains seven vents. The last unit, Qtbb4, has three vents aligned northwest-southeast on top of the main edifice. It is an interpretative choice to differentiate individual vents along the various fissures that make up the vent groupings observed at Table Butte, and other researchers may choose to represent each fissure as a single vent.

The Table Butte lavas were emplaced during two eruptive events. We interpret Qtbb1 as having been emplaced during an earlier event due to the change in mineralogy/petrology, spatial distribution, and apparent weathering of topography compared to the other lavas. Units Qtbb2, Qtbb3, and Qtbb4 make up the second event that formed the main edifice of Table Butte and the east-west fissure of The Breaks. While we prefer the hypothesis that the steep sided morphology of the main edifice is the result of burial of a phreatomagmatic eruption deposit, it remains possible that the shape is due to uplift from a magmatic intrusion.

This work improves the vent and event characterization of Table Butte and clarifies the styles of eruption involved in its development over time. As such, the results of this study contribute to improving the hazard assessment for the ESRP as a whole and the area near INL in particular.

Chapter 4: Discussion and Conclusion

4.1 - Geologic units

Table Butte is distinct from other volcanoes on the ESRP due to the unique environment in which the volcanic events occurred. The current 1:100,000 map of Table Butte places all basaltic rock into one unit (Kuntz et al., 1994). However, after close examination of the area, we conclude that there are four different rock units. The rock unit labels follow Qtbb1-4 with Q meaning Quaternary, tb for Table Butte, the last b for basalt, and the one-four signify the different rock units in age order. The first rock unit, Qtbb1, is distinct from the others due to the predominance of plagioclase crystals, which are up to 2 mm long and make up 6-10% of the hand sample, with trace olivine. This unit exposed outcrops in the Needle Butte trend and a north-south oriented portion of The Breaks west of the main Table Butte edifice. There is no radiometric age for Qtbb1, but superposition and morphology indicate that it is the oldest of the units studied. Qtbb2 includes only one location, deep erosional gullies on the northwest flank of Table Butte, the only area in which such gullies occur. Qtbb2 has over 20% olivine, approximately 2 mm across, and 2% plagioclase phenocrysts of the same size. Like Qtbb1, no dating or paleomagnetic work has been conducted for this rock unit. The next unit, Qtbb3, directly overlies Qttb2 on the main Table Butte edifice, extends south to the east-west trending portion of The Breaks, and includes trace ~2 mm plagioclase and olivine phenocrysts. Although Qtbb3 has not been dated directly, the unusual paleomagnetic signature measured from a sample collected in The Breaks indicates that it is from the same event as Qtbb4. The last layer, Qtbb4, contains trace plagioclase (up to 2 mm long) and ~5% olivine, primarily as individual phenocrysts up to 2 mm across. Qtbb4 was dated via ^{40}Ar-^{39}Ar by B. Turin to ~400 ka, with paleomagnetic results indicating that it is the same age as Qtbb3, which immediately overlies (D. Champion *pers. comm*.).

Although Qtbb3 and Qtbb4 were cautiously identified as separate units in the field based on their spatial relationship, the low crystallinity of both made it difficult to determine whether the apparent differences in phenocrysts was adequate to separate them from one another or consider them as two pulses within the same lava unit. This was done using point counting of thin sections and a comparison of major and minor elements measured by XRF. These measures, combined with the spatial context of the samples, revealed that Qtbb3 is a transitional unit between Qtbb1 and Qtbb4 and merits being treated separately from Qtbb4. Surprisingly, geochemical data for Qtbb2 indicated that it was entirely consistent with Qtbb4, despite its dramatically higher olivine content and being stratigraphically separated from that unit by Qtbb3.

4.2 – Paleohydrology

The phreatomagmatic explosion deposits alternating with dry spatter accumulation in The Breaks area suggest that there was surface water or groundwater available in the area ~400 ka. The modern water table exposed in Mud Lake and the nearby marshland is not anomalous in Table Butte's history; although there are no paleohydrology records dating back to nearly 400 ka, the Table Butte area has hosted multiple lakes over the last 17,000 years thanks to its location as a drainage basin and the existence of a shallow aquitard (Gianniny et al., 2002; Spinazola, 1994). The cycling between wet and dry layers exposed stratigraphically in The Breaks indicate that the phreatomagmatism during the eruption was water-limited, with dry fountaining serving as the dominant eruptive style.

Though eruption under a glacier can result in steep-sided, flat-topped volcanic landforms called tuyas, there is no evidence to support that glaciers ever reached the ESRP; they stayed in the mountain ranges to the north and south of the plain (G. Thackary, *pers. comm.*). Further, 400 ka was during a pronounced interglacial period (e.g., Cronin et al., 2019). Thus, it is likely that the water involved in the formation of Table Butte was in the form of shallow surface water or groundwater.

4.3- Table Butte vents

My field observations and mapping indicate a different number of vents than either the Hackett et al. (*in prep*) dataset or the one used by Gallant et al., (2019). I used the presence of near-vent spatter facies and landform morphology as my primary tools in identifying vents in the field. My current map, which treats each arcuate landform in The Breaks as a separate vent rather than combining them into linear fissures, identifies 18 vents on and around Table Butte. This substantial number of vents is still unusual for a volcano on the ESRP; however, this could be an issue of vent preservation because the unusual, steep-sided morphology of Table Butte reduces the likelihood of burial by the main edifice compared to typical low shield volcanoes nearby.

Qtbb1 included eight vents, five along the Needle Butte trend and another three in the north-south oriented section of The Breaks extending down to Clay Butte. The vents in The Breaks exhibit phreatomagmatic properties such as popcorn-like, low-vesicularity scoria, clay xenolith clasts, and rip-up clasts from older basalts. The location of the Qtbb2 vent is unknown due to burial by subsequent lavas; this is also true for Qtbb3 on the top of Table Butte, though that unit has seven vents in The Breaks. The last unit, Qtbb4, is associated with three vents on the top of Table Butte.

4.4 Geologic history

Qtbb1 erupted from fissures associated with the Needle Butte trend and the north-south linear feature in The Breaks, both west of the main Table Butte edifice. Although the Needle

Butte trend is consistent with dry, subaerial eruption, the Qtbb1 in The Breaks displays characteristics of alternating dry fountaining and phreatomagmatic blasting. The paleotopography prior to the eruptions is unknown, but it is possible that the change in external water effects could indicate that the ground was lower and wetter to the south in the area of The Breaks.

The earliest observed unit in the main Table Butte edifice is Qtbb2, exposed in deep gullies. This unit displays a greater degree of *in situ* weathering than the subsequent units and is characterized at the outcrop scale for having multiple meter-scale and thicker flow units, sometimes separated by glassy red cooling surfaces. I interpret Qtbb2 to be part of a package of eruptive units that contributed to the development of the steep-sided morphology of Table Butte. The increased degree of weathering observed in this unit could have been the result of water-lava interaction during emplacement that was inadequate to cause significant fragmentation. Although the relationship between Qtbb2 and external water is speculative, the concept of it, or lower, unobserved units, having had such interaction arises from a need to explain the anomalously steep sides of Table Butte given that the rest of the flank material appears to be unremarkable, *in situ*, low viscosity lava flows. I suggest that this package of units interacted with external water to create self-leveeing margins, or perhaps, under Qtbb2, even a tuff ring; note that Qttb2 itself was formed by lava and was not itself a tuff. Thus, I posit that the water-affected morphology, whether formed specifically by Qtbb2 or unit unobservable in the field, has been thinly covered by the subsequent eruption of Qtbb3 and Qtbb4, neither of which exhibit any evidence of water-lava interaction on the main Table Butte edifice. Qtbb3, however, does exhibit alternating periods of phreatomagmatic blasting and spatter-fed lava emplacement in the east-west trending area of The Breaks to the south. Taken with the similar distribution observed for Qtbb1, this further supports the idea of the larger Table Butte system essentially straddling a wet-dry margin during emplacement, with erupted materials in the north either being emplaced without the impact of external water or, in the case of my hypothesis for Qtbb2 and related unobserved flow units, eventually building up enough height to rise above the level of significant influence from external water.

Previous explanations for The Breaks, including my initial hypothesis, invoked rootless vents caused by lava from Table Butte flowing out over wet ground or shallow water (Hughes, *pers. comm.*; Kuntz, *pers. comm.*). Although the phreatomagmatic blast deposits accessible via a quarry on the southwestern corner of The Breaks could, in isolation, plausibly be explained as part of a rootless system, the predominance of fountain-fed welded spatter exposed in the interior walls of The Breaks provides key evidence that they were formed by a primary fissure. The spatter-fed flows extend the entire length of The Breaks, with weakly to profoundly welded layers exposed in the vertical section. The spatter commonly includes rip-up xenoliths of older basalt 5-15 cm across, recording extraction from depth and emplacement as ejecta; this is incompatible with spattering from a rootless system. Finally, the pyroclastic and spatter-fed lava units are approximately symmetric on either side of the long axis of their linear trend, supporting that the cratered zones were a source of magma rather than just a blasted front of a lava flow emanating from the main Table Butte edifice. As such, I interpret The Breaks as having been formed by alternating wet and dry eruptive phases from fissures intersecting a limited supply of surface or shallow groundwater.

Although I interpret that the overall morphology of Table Butte is the result of a buried unit that developed steep sides due to sudden cooling from external water effects, a competing hypothesis is that it may be instead of the result of upwarping over a cryptodome. There are several known cryptodomes on the ESRP, including Ferry Butte, Middle Butte, and Buckskin Butte (McCurry, and Welhan, 2012), with the last in the list having similar dimensions to Table Butte. Those buttes tend to show evidence of disrupted surfaces, whether through lid-like fracture patterns, tilted tops, or well-developed marginal gullies from erosion capitalizing on fractures caused by surface warping. Further, none of the confirmed cryptodomes have clear primary vents located on top of them. In contrast, there were no such fracture patterns or tilting observed at Table Butte, which also has three primary vents on top, and flow patterns from those vents are consistent with still being in their original position. In particular, the open channel drainage from the vent near the eastern margin of Table Butte's summit can be clearly followed, opening onto a broad lava flow unit spreading outwards on the flat ground beyond; shelly lava flow units exposed in the sidewalls of the channel appear to be *in situ*, without fractures or faults that would have likely formed during subsequent uplift via a cryptodome. Although these observations lead us to favor the buried-steep-sided-feature hypothesis, they do not offer a complete rejection of the possibility of a cryptodome. Further work via geophysical methods such as gravity and magnetic surveys could substantially clarify the accuracy of one hypothesis over the other; such efforts are outside of the scope of this work.

The $^{40}Ar/^{39}Ar$ data for Qtbb4 indicate that that unit was emplaced 392,000 years ago, and the unusual paleomagnetic signatures from Qtbb3 and Qtbb4 indicate that they have erupted during the same event. Although it is possible that all four units observed in the field were the result of a single volcanic event, I hypothesize that Qtbb1 was from a separate, earlier event based on its composition, the older softer morphology of the Qtbb1 portion of The Breaks, and its position in space and eruptive order compared to the other units. Additional ^{40}Ar-^{39}Ar dating or paleomagnetic analyses from Qtbb1 would be able to answer whether the collective Table Butte sequence included in this study was emplaced by one or more events.

4.5- Polygenetic or Distributed Volcanism

Despite my hypothesis that the units included in the Table Butte map were emplaced over two separate events, the volcano itself appears to be monogenetic. Qtbb1, the unit that I think may have occurred during a prior eruptive event, does not appear to actually contribute to the Table Butte edifice. As such, it is unreasonable to categorize Table Butte among the few known polygenetic volcanoes of the ESRP.

4.6- Summary of Responses to Hypotheses

Hypothesis One: Table Butte initially erupted subaqueously and transitioned into a subaerial eruption. The work presented here supports this hypothesis. Phreatomagmatic deposits were only observable in units that were lower in elevation and stratigraphy relative to the entirely to the Table Butte system. There is not yet a definitive answer to whether the main Table Butte edifice is shaped as it is due to an underlying phreatomagmatic deposit, but the orientation of surface flows, locations of vents, and lack of paleomagnetic deflection in samples taken from the flank suggest that this may be a more reasonable interpretation than a cryptodome. There are currently plans under way to use geophysical surveys to provide additional data.

Hypothesis Two: There are fewer vents than previously mapped, with perhaps as few as only five primary vents. Although my results support my initial hypothesis of there being fewer primary vents than in the Wetmore et al. (2009) dataset, there are still far more vents than I had anticipated. The predominance of dry spatter and spatter-fed lava from The Breaks areas and its symmetry around the axes of the crater chains are evidence in support of those vents being primary.

Hypothesis Three: Table Butte is a polygenetic volcano. Although I currently interpret the Table Butte system to have been emplaced over two events on the basis of geochemistry, vent locations, and qualitative interpretations of geomorphology, I would argue that the actual Table Butte volcano is not polygenetic. Given that the material associated with the first event is isolated to the Needle Butte Trend and the north-south oriented portion of The Breaks, it is unclear that it is appropriate to include that as the same volcano as the main Table Butte edifice. Further radiometric dating and paleomagnetic analyses are planned by the PVHA to shed additional light on the actual timing of the units studied here, and may even result in combining all of the Table Butte system into a single event.

4.7- Probabilistic Volcanic Hazards Assessment of the ESRP

The overarching motivation for updating the rock units, number of vents, and events at Table Butte was to improve the datasets available to the PVHA in their analysis of the ESRP. While the efforts of the PVHA extend well beyond the work covered in this thesis, my efforts have resulted in a higher vent density than what was previously mapped with aerial imagery (Fig. 4.1). Although my current interpretation is that Table Butte was emplaced over two events, thereby decreasing the recurrence interval for eruptions, this much be more thoroughly investigated through additional Ar/Ar dating and paleomagnetic analyses. In particular, it would be valuable to analyze samples from Qtbb1 and Qtbb2.

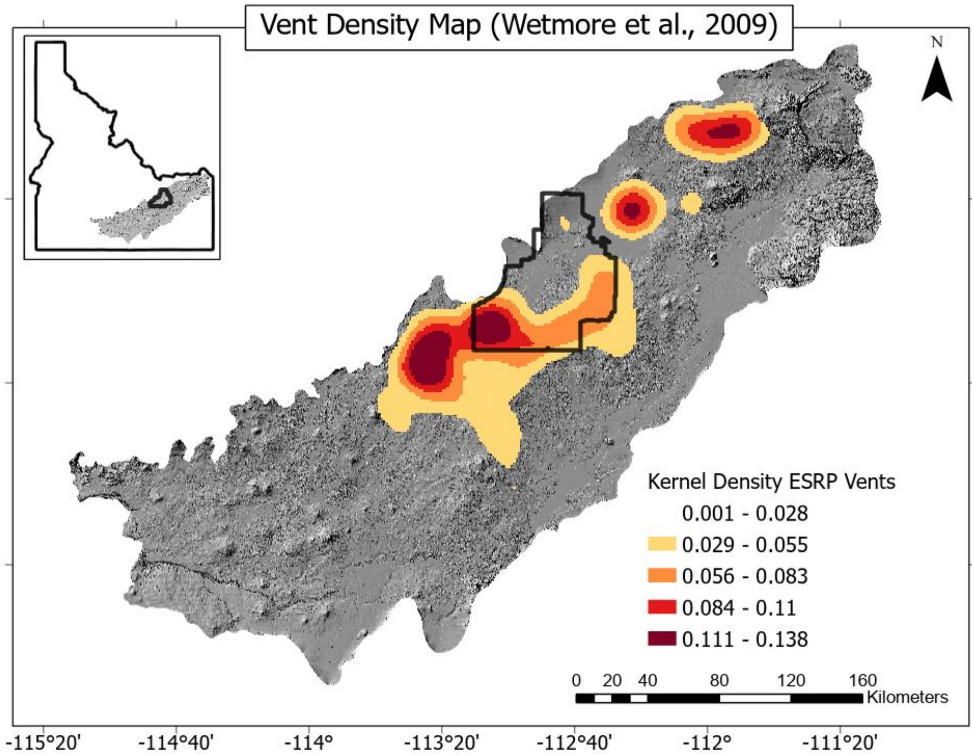
Vent Density Map (Wetmore et al., 2009)
N
44°
43°20'
42°40'
Kernel Density ESRP Vents
0.001 - 0.028
0.029 - 0.055
0.056 - 0.083
0.084 - 0.11
0.111 - 0.138
0 20 40 80 120 160
Kilometers
-115°20'
-114°40'
-114°
-113°20'
-112°40'
-112°
-111°20'

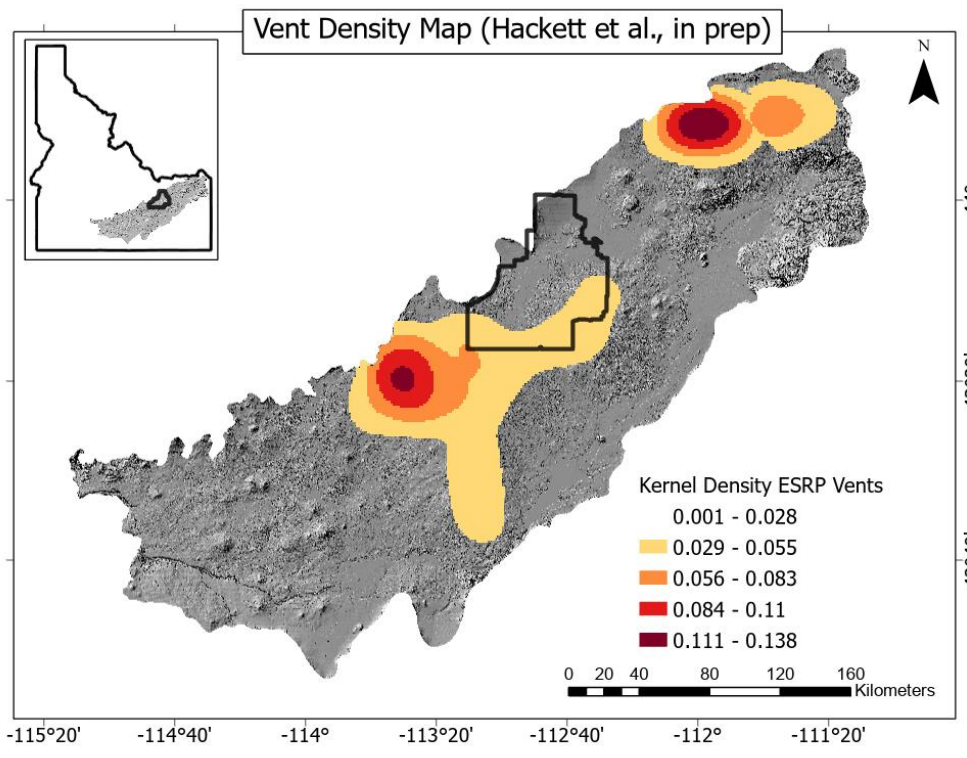
Vent Density Map (Hackett et al., in prep)
N
44°
43°20'
42°40'
Kernel Density ESRP Vents
0.001 - 0.028
0.029 - 0.055
0.056 - 0.083
0.084 - 0.11
0.111 - 0.138
0 20 40 80 120 160
Kilometers
-115°20'
-114°40'
-114°
-113°20'
-112°40'
-112°
-111°20'

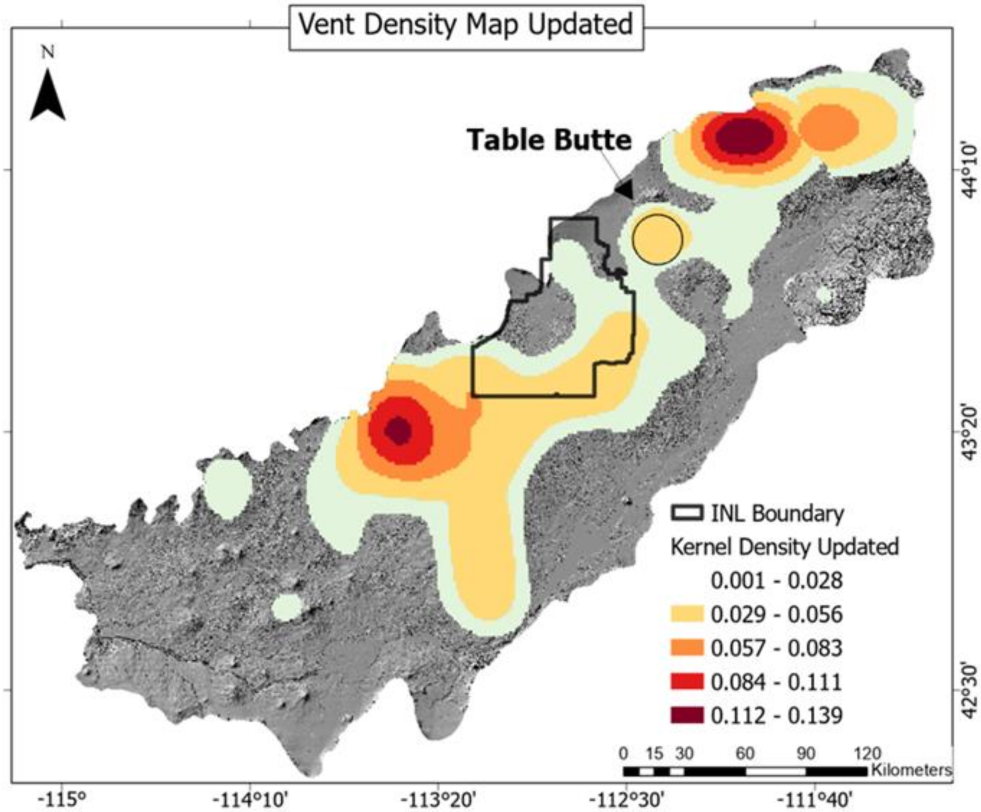

Figure 4.1: Vent density maps comparing Hackett et al. (in prep) vent dataset with the updated vent locations surrounding Table Butte.

4.8- Planetary Volcanology

In addition to volcanic hazards research, the improvements to the ESRP vent maps will also be useful for planetary volcanology. Planetary volcanology has changed significantly from a descriptive science to a quantitative approach using satellite imagery (Head and Wilson, 2022). In order to fully understand and correlate the properties found in satellite imagery, volcanologists use sites found on Earth that similarly represent the formation in the imagery. The ESRP already has a long tradition of being used in analog research to investigate Mars, the Moon, and other terrestrial bodies where plains-style volcanism is common (Hamilton et al., 2008; Head and Wilson, 2022; Hughes et al., 2019; Neish, et al., 2017; Tolometti et al., 2020). By improving the Table Butte portion of the ESRP vents map, we offer a better dataset to future researchers considering the spatial patterns of volcanism in other planetary settings, whether or not they are specifically interested in water-affected features like Table Butte.

4.9- Recommendations for Future Work

Further work at Table Butte should include additional radiometric dating, paleomagnetic analyses, corehole drilling, and geophysical surveys. Dating and paleomagnetic analyses of Qtbb1 and Qtbb2 would provide definitive insight into whether the Table Butte system was emplaced over more than one event. Although corehole would answer whether Table Butte's steep sides are the result of a cryptodome, it is unlikely that there will be adequate interest and funding to drill deeply enough. Instead, the cryptodome hypothesis could be studied using geophysical surveys. Both gravity and magnetic surveys could provide valuable clues while costing a fraction of drilling a corehole.

This work contributes to revising the geologic and vent maps for the ESRP and will help in the development of the first event map. These maps, once complete, will enable a more comprehensive study of ESRP volcanism than has ever been possible before. In addition to being used in the probabilistic volcanic hazard assessment being conducted by the INL, researchers will be able to investigate topics such as the correlation between magma chemistry and surface vent density or the changes in eruption characteristics over space and time.

References

Bartolini, S., Bolós, X., Martí, J., Pedra, E.R., and Planagumà, L., 2015, Hazard assessment at the Quaternary La Garrotxa Volcanic Field (NE Iberia): Natural Hazards, v. 78, p. 1349–1367, doi:10.1007/s11069-015-1774-y.

Barton, K.J., 2020, Links Between Eruptive Styles, Magmatic Evolution, and Morphology of Low-Shield Volcanoes: Snake River Plain, Idaho. [Theses and Dissertations]: Brigham Young University, v. 8612, p. 60, https://scholarsarchive.byu.edu/etd/8612.

Bebbington, M.S., 2013, Assessing Spatio-temporal eruption forecasts in a monogenetic volcanic field: Journal of Volcanology and Geothermal Research, v. 252, p. 14–28, doi: 10.1016/j.jvolgeores.2012.11.010.

Bonnichsen, B., White, C.M., and McCurry, M., 2002, Tectonic and Magmatic Evolution of the Snake River Plain Volcanic Province: Idaho Geological Survey, University of Idaho, Moscow, Idaho, Bulletin 30, 482 p., https://www.idahogeology.org/product/B-30.

Branney, M.J., Bonnichsen, B., Andrews, G.D.M., Ellis, B., Barry, T.L., McCurry, M., 2008, ‘Snake River (SR)-type’ volcanism at the Yellowstone hotspot track: distinctive products from unusual, high-temperature silicic super-eruptions: Bulletin of Volcanology: v. 70, p. 293-314. doi:10.1007/s00445-007-0140-7.

Champion, D.E., Hodges, M.K.V., Davis, L.C., and Lanphere, M.A., 2011, Paleomagnetic correlation of surface and subsurface basaltic lava flows and flow groups in the southern part of the Idaho National Laboratory, Idaho, with paleomagnetic data tables for drill cores: U.S. Geological Survey Scientific Investigations Report 2011-5049, p. 34.

Champion, D.E, and Kuntz, M.A., Unpublished geologic map of the Blackfoot 30 x 60-minute quadrangle, Idaho, scale 1:100,000.

Champion, D. E., Lanphere, M. A., & Kuntz, M. A., 1988. Evidence for a new geomagnetic reversal from lava flows in Idaho: Discussion of short polarity reversals in the Brunhes and late Matuyama polarity chrons. Journal of Geophysical Research: Solid Earth, 93(B10), 11667-11680.

Condit, C.D., and Connor, C.B., 1996, Recurrence rates of volcanism in basaltic volcanic fields: An example from the Springerville volcanic field, Arizona, Geologic Society of America Bulletin, v. 108, p. 1225-1241, doi:10.1130/0016-7606.

Connor, C.B., Condit, C.D., Crumpler, L.S., and Aubele, J.C., 1992, Evidence of regional structural controls on vent distribution: Springerville Volcanic Field, Arizona: Journal of Geophysical Research, v. 97, p. 12349–12359, doi:10.1029/92jb00929.

Connor, C. B., Conway, F. M., & Sigurdsson, H., 2000. Basaltic volcanic fields. *Encyclopedia of volcanoes*, *1*, 331-343.

Connor, C.B., Connor, L.J., Germa, A., Richardson, J.A., Bebbington, M., Gallant, E., and Saballos, J.A., 2019, How to use kernel density estimation as a diagnostic and forecasting tool for distributed volcanic vents: Statistics in Volcanology, v. 5, p. 1–25, doi:10.5038/2163-338x.4.3.

Cronin, T. M., Keller, K. J., Farmer, J. R., Schaller, M. F., O'Regan, M., Poirier, R.., & Santin, E. 2019. Interglacial paleoclimate in the Arctic. Paleoceanography and Paleoclimatology, 34(12), 1959-1979.

Dailey, S.R., 2016, Geochemistry of the flourine- and beryllium-rich Spor Mountain rhyolite, Western Utah: M.S. thesis, Brigham Young University, Provo, Utah

Deng, F., Connor, C.B., Malservisi, R., Connor, L.J., White, J.T., Germa, A., and Wetmore, P.H., 2017, A geophysical model for the origin of volcano vent clusters in a Colorado

Plateau volcanic field: Journal of Geophysical Research: Solid Earth, v. 122, p. 8910–8924, doi:10.1002/2017jb014434.

Esri. "Topographic" [basemap]. Scale Not Given. "World Topographic Map". February 19, 2012. http://www.arcgis.com/home/item.html?id=30e5fe3149c34df1ba922e6f5bbf808f. (May 25, 2017).

Forman S.L., and Pierson J., 2003, Formation of linear and parabolic dunes on the eastern Snake River Plain, Idaho in the nineteenth century: Geomorphology, v. 56, pp. 189-200, doi:10.1016/S0169-555X(03)00078-3.

Gallant, E., Richardson, J., Connor, C., Wetmore, P., Connor, L., 2018, A new approach to probabilistic lava flow hazard assessments, applied to the Idaho National Laboratory, eastern Snake River Plain, Idaho, USA: Geology, v. 46, p. 895–898, doi:10.1130/G45123.1.

Garwood, D.L., Kauffman, J.D., Othberg, K.L., Lewis, R.S., 2014, Geologic map of the Fairfield 30 x 60, minute quadrangle, Idaho: Idaho Geological Survey Geologic, Digital Web Map 171, scale 1:100,000.

Gianniny, G.L., Thackray, G.D., Kaufman, D.S., Forman, S.L., Sherbondy, M.J., and Findeisen, D., 2002, Late Quaternary highstand in the Mud Lake and Big Lost Trough subbasins of Lake Terreton, Idaho *in* Link, P.K., and Mink, L,L., eds., Geology, Hydrogeology, and Environmental Remediation: Idaho National Engineering and Environmental Laboratory, Eastern Snake River Plain, Idaho: Boulder, Colorado: Geologic Society of America Special Paper, v. 353, p. 77-90.

Greeley, R., 1982, The Snake River Plain, Idaho: Representative of a new category of volcanism: Journal of Geophysical Research, v. 87, B4, p. 2705-2712.

Grosse. P., Ramacciotti, M.L.O., Fochi, F.E., Guzman, S., Orihashi, and Y., Sumino, H., 2020, Geomorphology, morphometry, spatial distribution and ages of mafic monogenetic volcanoes of the Peinado and Inchauasi fields, southernmost Central Volcanic Zone of the Andes: Journal of Volcanology and Geothermal Research, v. 401, p. 1-23, doi:10.1016/j.jvolgeores.2020.106966.

Hackett, W.R., Smith, R.P., and Khericha, S., 2002, Volcanic hazards of the Idaho National Engineering and Environmental Laboratory, southeast Idaho, *in* B. Bonnichsen, C.M. White, and M. McCurry, eds., Tectonic and Magmatic Evolution of the Snake River Plain Volcanic Province: Idaho Geological Survey Bulletin 30, p. 461-482.

Hamilton, V.E., Morris, R.V., Gruener, J.E., and Mertzman, S.A., 2008, Visible, near-infrared, and middle infrared spectroscopy of altered basaltic tephras: Spectral signatures of phyllosilicates, sulfates, and other aqueous alteration products with application to the mineralogy of the Columbia Hills of Gusev Crater, Mars: Journal of Geophysical Research: Planets, v. 113, p. 1-30, doi:10.1029/2007je003049.

Head, J.W., and Wilson, L., 2022, Planetary volcanology: progress, problems, and opportunities, Bulletin of Volcanology, vol. 84, p. 1-10.

Hughes, S.S., Haberle, C.W., Kobs-Nawotniak, S.E., Sehike, A., Garry, W.B., Elphic, R.C., Payler, S.J., Stevens, A.H., Cockell, C.S., Brady, A.L., Heldmann, J.L., Lim, D.S.S., 2019, Basaltic terrains in Idaho and Hawaii as planetary analogs for Mars geology and astrobiology: Astrobiology, v. 19, p. 260–283, doi:10.1089/ast.2018.1847.

Hughes, S.S., Wetmore, P.H., and Casper, J.L., 2002, Evolution of Quaternary tholeiitic basalt eruptive centers on the eastern Snake River Plain, Idaho, *in* Bonnichsen, B., White, C.

M., and McCurry, M., eds., Tectonic and Magmatic Evolution of the Snake River Plain Volcanic Province: Idaho Geological Survey Bulletin 30, p. 363-385.

Hughes, S.S., Smith, R.P., Hackett, W.R., and Anderson, S.R., 1999, Mafic Volcanism and Environmental Geology of the Eastern Snake River Plain, Idaho, *in* Hughes, S.S., and Thackray, G.D., eds., Guidebook to the Geology of Eastern Idaho: Idaho Museum of Natural History, p. 143-168.

Hughes, S.S., Kobs-Nawotniak, S.E., Sears, D.W.G., Borg, C., Garry, W.B., Christiansen, E.H., Haberle, C.W., Lim, D.S.S., Heldmann, J.L., 2018, Phreatic explosions during basaltic fissure eruptions: Kings Bowl lava field, Snake River Plain, USA: Journal of Volcanology and Geothermal Research, v. 351, p. 89-104, doi:10.1016/j.jvolgeores.2018.01.001.

Hughes, S.S., and McCurry, M., 2002, Bulk major and trace element evidence for a time-space evolution of Snake River Plain rhyolites, Idaho, *in* Bonnichsen, B., White, C.M., and McCurry, M., eds., Tectonic and Magmatic Evolution of the Snake River Plain Volcanic Province: Idaho Geological Survey Bulletin 30, p. 161-176.

Humphreys, E.D., Dueker, K., Schutt, D., and Saltzer, R., 1999, Lithosphere and asthenosphere structure and activity in Yellowstone's wake: Geological Society of America Abstracts with Programs, v. 31, p. A17.

Jain, A. K. 2009. "Data Clustering: 50 years beyond K-Means." Pattern Recognition Letters.

Jones, T.J., Houghton, B.F., Llewellin, E.W., Parcheta, C.E., and Höltgen, L., 2018, Spatter matters – distinguishing primary (eruptive) and secondary (non-eruptive) spatter deposits: Scientific Reports, v. 8, p. 9179, doi:10.1038/s41598-018-27065-1.

Kuntz, M.A., 1979, Geologic map of the Juniper Buttes area, eastern Snake River Plain, Idaho, USGS Miscellaneous Investigations Series Map I-1115, scale 1:48000.

Kuntz, M.A., Covington, H.R., Schorr, L.J., 1992, An overview of basaltic volcanism of the eastern Snake River Plain, Idaho. In: Link, P.K., Kuntz, M.A., Platt, L. (eds) Regional geology of eastern Idaho and western Wyoming. Geol Soc Am Mem 179:227–267.

Kuntz, M.A., Skipp, B.A., Lanphere, M.A., Scott, W.E., Pierce, K.L., Dalrymple, G.B., Champion, D.E., Embree, G.F., Page, W.R., Morgan, L.A., Smith, R.P., Hackett, W.R., & Rodgers, D.W., 1994. Geologic map of the Idaho National Engineering Laboratory and adjoining areas, eastern Idaho.

Kuntz, M.A., (*unpublished*), Geologic map of the Circular Butte 30 x 60 minute quadrangle, Idaho: Idaho Geological Survey, scale 1:100,000.

Kuntz, M.A., Geslin, J.K., Mark, L.E., Hodges, M.K.V., Kauffman, M.E., Champion, D.E., Lanphere, M.R., Rodgers, D.W., Anders, M.H., Link, P.K., and Boyack, D.L., 2003, Geologic map of the northern and central parts of the Idaho National Engineering and Environmental Laboratory, eastern Idaho: Idaho Geological Survey Geologic Map 35, scale 1:50,000.

Kuntz, M.A., Skipp, B., Champion, D.E., Gans, P.B., Van Sistine, D.P., and Snyders, S.R., 2007, Geologic map of the Craters of the Moon 30’ x 60’ quadrangle, Idaho: U.S. Geological Survey Scientific Investigations Map SIM-2969, 64 p., scale 1:100,000

Kuntz, M.A., Champion, D.E., Turrin, B.R., Gans, P.B., Covington, H.R., and VanSistine, D.P., 2018, Geologic map of the north half of the Lake Walcott 30'×60' quadrangle, Idaho: U.S. Geological Survey Scientific Investigations Report 3405, pamphlet 25 p., scale 1:100,000, https://doi.org/10.3133/sim3405.

Leeman, W.P., Annen, C., and Dufek, J., 2007, Snake River Plain – Yellowstone volcanism: implications for magma genesis and magma fluxes. The Geological Society of London Special Publication 304, p. 235–259, doi: 10.1144/SP304.12.

Link, P.K., and Stanford, L.R., 1999, Geologic map compilation of the Pocatello 30 x 60-minute quadrangle, Idaho: Idaho Geological Survey Technical Report 99-2, scale 1:100,000.

Lisiecki, L.E., and Raymo, M.E., 2005, A Pliocene-Pleistocene stack of 57 globally distributed benthic d18O records, Paleoceanography, v. 20, PA1003, doi:10.1029/2004PA001071.

McCurry, M., Hayden, K.P., Morse, L.H., Merzman, S., 2008, Genesis of post-hotspot, A-type rhyolite of the Eastern Snake River Plain volcanic field by extreme fractional crystallization of olivine tholeiite. *Bull Volcanol* 70, 361–383. https://doi.org/10.1007/s00445-007-0143-4

McCurry, M., and D. Rodger (2009), Mass transfer along the Yellowstone hot spot track I: Petrologic constraints on the volume of mantle-derived magma, J. Volcanol. Geotherm. Res., 188, 86–98, doi:10.1016/j.jvolgeores.2009.04.001.

McCurry, M., & Welhan, J., 2012, Do Magmatic-related geothermal energy resources exist in southeast Idaho. *GRC Transactions, 36*, 699-707.

McQuarrie, N., and Rodgers, D.W., 1998, Subsidence of a volcanic basin by flexure and lower crustal flow: The eastern Snake River Plain, Idaho: Tectonics, v. 17, no. 2, p. 203-220.

Michon, L., and Merle, O., 2001, The evolution of the Massif Central rift: spatio-temporal distribution of the volcanism. Bulletin de a Société Géologique de France, v. 172, p. 201-211, doi:10.2113/172.2.201.

Morse, L.H., and McCurry, M., 2002, Genesis of alteration of Quaternary basalts within a portion of the eastern Sanke River Plain aquifer, in Link, P.K., and Mink, L.L., eds., Geology, Hydrology, and Environmental Remediation: Idaho National Engineering and Environmental Laboratory, Eastern Snake River Plain, Idaho: Boulder, Colorado, Geological Society of America Special Paper 353, p. 213-224.

Neish, C.D., Hamilton, C.W., Hughes, S.S., Kobs-Nawotniak, S., Garry, W.B., Skok, J.R., Elphic, R.C., Schaefer, E., Carter, L.M., Bandfield, J.L., Osinski, G.R., Lim, D., Heldmann, J.L., 2017, Terrestrial analogues for lunar impact melt flows: Icarus, v. 281, p. 73–89, doi:10.1016/j.icarus.2016.08.008.

Németh, K., and Kósik, S., 2020, Review of Explosive Hydrovolcanism, Geosciences, v. 10, p. 1-27, doi: 10.3390/geosciences10020044.

Othberg, K.L, Kauffman, J.D., Gillerman, V.S., and Garwood, D.L., 2012, Geologic map of the Twin Falls 30 x 60, minute quadrangle, Idaho: Idaho Geological Survey Geologic, Map 49, scale 1:100,000.

Pierce, K.L., Morgan, L.A., and Saltus, R.W., 2002, Yellowstone plume head: Postulated tectonic relations to the Vancouver slab, continental boundaries, and climate, *in* Bonnichsen, B., White, C.M., and McCurry, M., eds., Tectonic and Magmatic Evolution of the Snake River Plain Volcanic Province: Idaho Geological Survey Bulletin 30, p. 5-33.

Potter, K.E., Champion, D.E., Duncan, R.A., Shervais, J.W., 2019, Volcanic stratigraphy and age model of the Kimama deep borehole (Project Hotspot): Evidence for 5.8 million years of continuous basalt volcanism, central Snake River Plain, Idaho. Geosphere, v. 15 (3) p. 736–758. doi: https://doi.org/10.1130/GES01679.1

Rodgers, D.W., Ore, H.T., Bobo, R.T., McQuarrie, N., and Zentner, N., 2002, Extension and subsidence of the eastern Snake River Plain, Idaho, *in* Bonnichsen, B., White, C.M., and

McCurry, M., eds., Tectonic and Magmatic Evolution of the Snake River Plain Volcanic Province: Idaho Geological Survey Bulletin 30, p. 121-155.

Silverman, B. W. *Density Estimation for Statistics and Data Analysis*. New York: Chapman and Hall, 1986.

Skilling, I.P., White, J.D.L., and McPhie, J., 2002, Peperite: a review of magma-sediment mingling, Journal of Volcanology and Geothermal Research, vol. 114, p. 1-17.

Skipp, Betty, and M.A. Kuntz, 2009, Geologic map of the Arco 30 x 60-minute quadrangle, south-central Idaho: Idaho Geological Survey Geologic Map 47, 42 p., scale 1:100,000.

Smith, I.E.M., Nemeth, K., 2017. Source to surface model of monogenetic volcanism: a critical review. Geologic Society of London., Spec. Publ. v. 446, p 1-28, doi:10.1144/SP446.14

Spinazola, J.M., 1994, Geohydrology and simulation of flow and water levels in the aquifer system in the Mud Lake area of the eastern Snake River Plain, Eastern Idaho: U.S. Geological Survey Water-Resources Investigations Report 93-4227, p. 78.

Stearns, H.T., Bryan, L.L., and Crandall, L., 1939, Geology and water resources of the Mud Lake region, Idaho, including the Island Park area: U.S. G.P.O., Water Supply Paper 818, https://pubs.er.usgs.gov/publication/wsp818.

Stroncik, N.A., and Schmincke, H., 2001, Evolution of palagonite: Crystallization, chemical changes, and element budget: Geochemistry, Geophysics, Geosystems, v. 2, p. 1-43, doi:10.1029/2000gc000102.

Tolometti, G.D., Neish, C.D., Osinski, G.R., Hughes, S.S., and Nawotniak, S.E.K., 2020, Interpretations of lava flow properties from radar remote sensing data: Planetary and Space Science, v. 190, p. 104991.

Twining, B.V., and Bartholomay, R.C., 2011, Geophysical logs and water-quality data collected for boreholes Kimama-1A and -1B, and a Kimama water supply well near Kimama, southern Idaho: U.S. Geological Survey Data Series 622 (DOE/ID 22215), 18 p., plus appendix.

U.S. Geological Survey, 2019, 3D Elevation Program 10-Meter Resolution Digital Elevation Model (published 20200606), accessed October 2020, at URL https://www.usgs.gov/core-science-systems/ngp/3dep/data-tools

Van der Plas, L., and Tobi, A.C., 1965. A chart for judging the reliability of point counting results. American Journal of Science, v. 263(1), p. 87-90.

Wetmore, P.W., Hughes, S.S., Connor, L.J., Caplinger, M.L., and Connor, L.J., 2009. Spatial distribution of eruptive centers about the Idaho National Laboratory, *in* Connor, C.B., Chapman, N.A., eds., Volcanic and Tectonic Hazard Assessment for Nuclear Facilities. Cambridge University Press, pp. 385–405.

Wohletz, K.H., 1986, Explosive magma-water interactions: Thermodynamics, explosion mechanisms, and field studies: Bulletin of Volcanology, vol. 48, p. 245-264.

Wohletz, K.H., and Sheridan, M.F., 1983, Hydrovolcanic explosions; II, Evolution of basaltic tuff rings and tuff cones: American Journal of Science, v. 283, p. 385–413, doi:10.2475/ajs.283.5.385.

Wright, K.E., McCurry, M., and Hughes, S.S., 2002, Petrology and geochemistry of the Miocene tuff of McMullen Creek, central Snake River Plain, Idaho, in Bonnichsen, B., White, C.M., and McCurry, M., eds., Tectonic and Magmatic Evolution of the Snake River Plain Volcanic Province: Idaho Geological Survey Bulletin 30, p. 177-194.

Zarazúa-Carbajal, M.C., and Cruz-Reyna, S.D. la, 2020, Morpho-chronology of monogenetic scoria cones from their level contour curves. Applications to the Chichinautzin monogenetic field, Central Mexico: Journal of Volcanology and Geothermal Research, v. 407, p. 107093, doi:10.1016/j.jvolgeores.2020.107093.

Zimanowski, B., Büttner, R., Lorenz, V., and Häfele, H., 1997, Fragmentation of basaltic melt in the course of explosive volcanism: Journal of Geophysical Research: Solid Earth, v. 102, p. 803–814, doi:10.1029/96jb02935.